

TALLINN UNIVERSITY OF TECHNOLOGY
School of Information Technologies

Toomas Erik Anijärv, 207636IAHM

**Long-term electrophysiological changes and
relationship with clinical and biochemical
measures following a 6-week low-dose oral
ketamine treatment in adults with major
depressive disorder and chronic suicidality**

Master's thesis

Supervisors: Prof. Jim Lagopoulos,
PhD
Prof. Maie Bachmann,
PhD

Tallinn 2023

TALLINNA TEHNIKAÜLIKOOL
Infotehnoloogia teaduskond

Toomas Erik Anijärv, 207636IAHM

**Pikaajalised elektrofüsioloogilised muutused
ning seos kliiniliste ja biokeemiliste teguritega
pärast 6-nädalast suukaudset ketamiiniravi
depressiooni ja enesetapumõtetega
täiskasvanutel**

Magistritöö

Juhendajad: Prof. Jim Lagopoulos,
PhD
Prof. Maie Bachmann,
PhD

Tallinn 2023

Author's declaration of originality

I hereby certify that I am the sole author of this thesis. All materials, references to the literature and the work of others have been referred to. This thesis has not been presented for examination anywhere else, however (i) as this study is a follow-up to a pilot study at the Thompson Institute of University of the Sunshine Coast [1], the used data was not collected/recorded by me; (ii) most of the results have also been published in a journal article where I am a co-first author [2] (added the citation on 18.02.2023). The source code created for data preparation and analysis is available on my personal GitHub named as 'EEG-pyline' [3].

Author: Toomas Erik Anijärv

03.01.2023

Abstract

Aims: This thesis investigates electrophysiological changes and relationship with clinical and biochemical measures in depressive and suicidal patients during and following a 6-week low-dose oral ketamine treatment using electroencephalography (EEG) spectral analysis. Previous studies have found low-dose ketamine to be effective in alleviating clinical symptoms and inducing electrophysiological changes, but to our knowledge, this is the first study investigating these changes and correlation with clinical and biochemical measures in long term, i.e., during the 6-week treatment period and 4 weeks after.

Methods: Participants were diagnosed with major depressive disorder (MDD) and chronic suicidality. 4-minutes eyes closed resting EEG was recorded (N=25); blood tests were collected for biochemical measurements (N=20). Data analysis pipeline was created using the most recent methods and tools with an aim to create a semi-automated and time-saving solution to prepare EEG data for analysis. Spectral analysis was performed using Welch's power spectrum density (PSD) method. Theta, alpha, low-beta, and high-beta band powers were calculated at frontal, temporal, centro-parietal, and occipital regions. Correlation analysis was conducted using Spearman's method.

Results: Spectra changes were prominent in theta, alpha, and low-beta bands. Ketamine treatment significantly decreased alpha band power at centro-parietal region during the treatment but normalised back to baseline level after the treatment had stopped, suggesting that the effects of ketamine treatment to be transient in terms of alpha activity. However, power changes in centro-parietal, temporal and occipital theta; temporal alpha; temporal and occipital low-beta occurred after the treatment had ended, which could be explained by possible delayed ketamine-induced neuroplastic changes. Theta band changes displayed significant correlations with Depression Anxiety Stress Scale 21 (DASS). Beck Scale for Suicidal Ideation (BSS) had no correlation with band power changes. Brain-derived neurotrophic factor (BDNF) correlated with theta band changes after the treatment had stopped and interleukin 6 (IL-6) with alpha band during the treatment. Endothelin 1 (ET-1) did not correlate with any significant band power changes.

This thesis is written in English and is 29 pages long, including 6 chapters, 18 figures and 14 tables.

Annotatsioon

Eesmärgid: Käesolev lõputöö uurib depressiooni ja enesetapumõtetega täiskasvanute elektrofüsioloogilisi muutusi ja nende seost kliiniliste ja biokeemiliste teguritega 6-nädalase suukaudse ketamiiniravi jooksul, kasutades elektroentsefalograafia (EEG) spektraalanalüüsi. Varasemad uuringud on tõendanud ketamiiniravist tulenenud kliiniliste sümptomite leevendamist ja elektrofüsioloogilisi muutusi, kuid antud lõputöö uurib esmakordselt ketamiinist tulenevaid elektrofüsioloogilisi muutusi ja suhet kliiniliste ja biokeemiliste teguritega pikaajaliselt.

Meetodid: Uuringust osavõtjatel oli diagnoositud kliiniline depressioon (MDD) ja krooniline suitsiidsus. Silmad kinni puhkeoleku EEG salvestus kestis neli minutit (N=25) ning võeti vereproovid biokeemiliste muutujate saamiseks (N=20). Töö käigus kasutati uusimaid meetodeid ja tööriistu eesmärgiga luua poolautomaatne ja aega säästev lahendus EEG andmete eeltötluseks ja analüüsiks. Uuritav aju jaotati regiooniti neljaks sagaraks: otsmikusagar, oimusagar, tsentro-parietaalsagar ja kuklasagar. Spektraalanalüüs teostati Welch'i võimsuse spektraaltiheduse (PSD) meetodiga. Võimsus leiti neljast erinevast sagedusribast: teeta, alfa, madal beeta ja kõrge beeta. Korrelatsioonid kalkuleeriti Spearmani meetodiga.

Tulemused: Ketamiiniravi tõi esile muutused teeta, alfa ja madala beeta sagedusribades. Tsentro-parietaalse alfa võimsus vähenes raviperioodi ajal, kuid normaliseerus pärast ravi lõppu, näidates ketamiini mõju mööduvust. Teistes sagedusribades (tsentro-parietaalne, oimu ja kukla teeta; oimu alfa; oimu ja kukla madal beeta) toimusid muutused ainult pärast raviperioodi lõppu, mida võib seletada ketamiinist põhjustatud võimalike hilinevad neuroplastiliste muutustega. Teeta riba muutused näitasid märkimisväärset korrelatsiooni depressiooni-ärevuse-stressi skaalaga (DASS), kuid Becki enesetapumõtete skaalal (BSS) ei korreleerunud ühegi sagedusriba võimsuse muutusega. Tserebraalne neurotroofne faktor (BDNF) korreleerus teeta riba muutustega pärast ravi lõppu ja interleukiin 6 (IL-6) alfa ribaga ravi ajal. Endoteliin 1 (ET-1) ei olnud korrelatsioonis ühegi sagedusriba statistiliselt olulise võimsuse muutusega.

Lõputöö on kirjutatud inglise keeles ning sisaldab teksti 29 leheküljel, 6 peatükki, 18 joonist, 14 tabelit.

List of abbreviations and terms

AMPA	α -amino-3-hydroxy-5-methyl-4-isoxazolepropionic acid
AR	Autoreject
BDNF	Brain-derived neurotrophic factor
BPD	Borderline personality disorder
BSS	Beck Scale for Suicidal Ideation
CV	Cross-validation
DASS	Depression Anxiety Stress Scale 21
DSM-5	Diagnostic and Statistical Manual of Mental Disorders 5th ed.
eEF2	Eukaryotic elongation factor 2
EEG	Electroencephalography
EOG	Electrooculography
ET-1	Endothelin 1
FIR	Finite impulse response
GABA	γ -aminobutyric acid
GAD	Generalised anxiety disorder
IL-6	Interleukin 6
IQR	Interquartile range
M	Median
MAD	Median absolute deviation
MDD	Major depressive disorder
mTORC1	Mammalian target of rapamycin complex 1
NMDA	N-methyl-D-aspartate
OKTOS	Oral Ketamine Trial on Suicidality
PSD	Power spectrum density
PTSD	Post-traumatic stress disorder
SD	Standard deviation
SUD	Substance use disorder
TrkB	Tropomyosin receptor kinase B

Table of contents

1 Introduction	11
2 Background.....	14
2.1 Major depressive disorder (MDD) and suicidality	14
2.2 Ketamine.....	14
2.2.1 Clinical applications	14
2.2.2 Neurobiological mechanisms	15
2.3 Electroencephalography	16
2.3.1 Neuronal activity	16
2.3.2 Frequency domain analysis	17
2.3.3 Signal artefacts and noise	18
2.4 Biochemistry.....	19
2.4.1 Brain-derived neurotrophic factor	19
2.4.2 Interleukin 6.....	20
2.4.3 Endothelin 1.....	20
3 Methodology.....	21
3.1 Study design	21
3.1.1 Clinical trial	21
3.1.2 Participants	22
3.2 Data acquisition	22
3.2.1 Electrophysiological recordings	22
3.2.2 Blood testing.....	23
3.3 Electroencephalographic analysis.....	23
3.3.1 Signal pre-processing	24
3.3.2 Spectral analysis	26
3.4 Correlation analysis	28
3.5 Statistics.....	28
4 Results	29
4.1 Changes in band powers	29
4.1.1 Theta band	29

4.1.2 Alpha band.....	30
4.1.3 Low-beta band	30
4.1.4 High-beta band	31
4.2 Correlation with clinical outcomes.....	32
4.3 Correlation with biochemical measures	33
5 Discussion.....	35
6 Summary.....	38
References	39
Appendix 1 – Non-exclusive licence for reproduction and publication of a thesis.....	45
Appendix 2 – Demographics table of the participants	46
Appendix 3 – Tables for band powers and comparisons across timepoints.....	47
Appendix 4 – Correlation tables between band powers and clinical outcomes	49
Appendix 5 – Correlation tables between band powers and biochemical measures	51

List of figures

Figure 1. Antidepressant effects of ketamine are hypothesised to take place via two different pathways	16
Figure 2. Fundamental logic of EEG measurement	17
Figure 3. Commonly used predefined frequency bands and their EEG signals in time domain	18
Figure 4. EEG signal artefacts and noise.....	19
Figure 5. Clinical trial time schedule.....	21
Figure 6. Electrode placement for BioSemi ActiveTwo 32-channel system	23
Figure 7. Amplitude response in frequency-domain of the designed filter.....	25
Figure 8. Artefact rejection process by Autoreject algorithm	26
Figure 9. Global Field Power plots of one participant’s EEG signals before and after artefact rejection.	26
Figure 10. An example of the manual signal reliability check step via topographical plots	27
Figure 11. Flowchart of the EEG pipeline starting from pre-processing and ending with spectral analysis.....	27
Figure 12. Theta band power for different timepoints and brain regions.....	29
Figure 13. Alpha band power for different timepoints and brain regions	30
Figure 14. Low-beta band power for different timepoints and brain regions.....	31
Figure 15. High-beta band power for different timepoints and brain regions.....	32
Figure 16. Theta at occipital region between post-treatment and follow-up timepoints correlates positively with DASS-D and DASS-S.....	33
Figure 17. At centro-parietal region, theta between post-treatment and follow-up timepoints correlates negatively with BDNF and alpha between baseline and post-treatment correlates positively with IL-6.....	34
Figure 18. Illustrative visualisation of brain regions and significant changes in band powers between baseline and post-treatment and between post-treatment and follow-up timepoints	36

List of tables

Table 1. Filter parameters.....	24
Table 2. Demographics, diagnosis, concurrent medications, and gathered data of the subjects	46
Table 3. Theta band power descriptive values for different timepoints and brain regions with statistical significance levels for comparisons	47
Table 4. Alpha band power descriptive values for different timepoints and brain regions with statistical significance levels for comparisons	47
Table 5. Low-Beta band power descriptive values for different timepoints and brain regions with statistical significance levels for comparisons.....	47
Table 6. High-Beta band power descriptive values for different timepoints and brain regions with statistical significance levels for comparisons.....	48
Table 7. Theta band power correlation coefficients with clinical outcomes for different timepoints and brain regions.....	49
Table 8. Alpha band power correlation coefficients with clinical outcomes for different timepoints and brain regions.....	49
Table 9. Low-beta band power correlation coefficients with clinical outcomes f for different timepoints and brain regions.....	49
Table 10. High-beta band power correlation coefficients with clinical outcomes for different timepoints and brain regions.....	50
Table 11. Theta band power correlation coefficients with biochemical measures for different timepoints and brain regions.....	51
Table 12. Alpha band power correlation coefficients with biochemical measures for different timepoints and brain regions.....	51
Table 13. Low-beta band power correlation coefficients with biochemical measures for different timepoints and brain regions.....	51
Table 14. High-beta band power correlation coefficients with biochemical measures for different timepoints and brain regions.....	52

1 Introduction

Major depressive disorder (MDD) is one of the most prevalent and disabling psychiatric disorders in the world, affecting one in six adults in their lifetime [4]. Besides the significant burden conferred by MDD alone, evidence suggests it can be a preliminary condition to many other psychiatric illnesses and is a major risk factor for suicidal ideation [4]. Clinically, suicidal ideation is commonly associated with recurrent and intrusive contemplations, wishes, and preoccupations with death and suicide. Annually, more than 700,000 deaths are attributed to suicide [5], which due to the high prevalence in MDD, substantially contributes to the 10.6 and 7.2 life years lost in men and women, respectively [6]. Currently, the clinical diagnosis and suicidal ideation rely on self-report measures in combination with psychiatrist screening within the confines of the Diagnostic and Statistical Manual of Mental Disorders 5th edition (DSM-5) criteria [7], which both are subjective in nature. To establish more robust diagnostic certainty that can address the significant variability in disorder pathogenesis and presentation, significant research has been focused on finding biomarkers for neuropsychiatric disorders (including MDD and suicidality) as reviewed in [8]–[10].

Previously, structural and functional brain abnormalities have formed the primary focus of biomarker identification in MDD [11] and suicidality [12]. Recently, there has been increasing interest in how these changes relate to dysfunctional neural circuit dynamics in suicidality [13] and MDD [14]. The spatio-temporal profile of neural circuit dynamics, and therefore information processing within the brain, is predominantly defined by the dynamic balance of excitatory and inhibitory transmission [15]. An emergent property of excitatory and inhibitory neural transmission that lends itself to measurement is the synchronised activity that arises from populations of neurons [16]. Electroencephalography (EEG) is a non-invasive imaging modality frequently used to measure these brain activity signals [17], which owing to technological advancements, has garnered renewed interest as a valuable method for determining biomarkers for MDD [8]–[10]. In recent clinical studies, EEG has shown promise in classifying depressed (and

suicidal) patients from healthy individuals [18]–[21] and in assessing ketamine as treatment for depression [22], [23].

Ketamine, a non-competitive N-methyl-D-aspartate (NMDA) receptor antagonist, has shown considerable therapeutic potential in alleviating symptoms of MDD and suicidality at low-doses (0.5 mg/kg; reviewed in [24]). Mechanistically, these effects are associated with NMDA receptor mediated changes in excitatory and inhibitory transmission in the medial pre-frontal cortex, anterior cingulate cortex, and hippocampus [25], driving a period of plasticity-induced structural and functional remodelling [26].

One of the most common techniques to acquire information from EEG data is to transform the signals from time domain to frequency domain and describe the power of signals within well-known frequency bands: delta, theta, alpha, beta, and gamma [8]. This method, called band power or spectral analysis, of both global and region-specific EEG signals formed from cortical and sub-cortical circuits has yielded valuable insight into the influence of ketamine on neural circuit dynamics. One study compared 111 depressed and 526 healthy subjects, and found increased power in theta, alpha, and beta bands at parietal and occipital regions for the depressed group [18]. In addition, increased relative theta band power has been found in healthy individuals with higher suicidality in frontal and central regions [20]. Furthermore, alpha band power has been found to be greater in frontal and parietal regions for unmedicated MDD patients compared with healthy controls [19]. A recent randomised double-blind trial including participants with treatment-resistant MDD found that intravenous sub-anaesthetic (0.5mg/kg) ketamine decreased power in theta, alpha (parietal region), and beta (centro-parietal region) bands shortly after infusion while decreasing depressive symptoms and suicidal ideation [23]. However, in contrast, another study found alpha band power to be increased at pre-frontal region early after sub-anaesthetic ketamine infusion for participants with treatment-resistant depression [22].

This study aims to identify changes in the spectral properties of EEG after a 6-week oral ketamine treatment and determine if there are any correlations between EEG spectral results and clinical/biochemical measures, clinical outcomes included self-reported questionnaires, Beck Scale for Suicidal Ideation (BSS) and Depression Anxiety Stress Scale 21 (DASS). Biochemical measures included brain-derived neurotrophic factor (BDNF), interleukin 6 (IL-6), and endothelin 1 (ET-1). Considering previous findings in

[18]–[20], [22], [23], it was hypothesised that compared to baseline, EEG patterns at the post-treatment (6-week) timepoint would show; 1) a significant decrease of theta band power in all regions (frontal, temporal, centro-parietal, occipital), 2) a decrease of alpha band power in centro-parietal region, and 3) a decrease of low- and/or high-beta band power in centro-parietal region. At the final follow-up timepoint (10-week), it was predicted that the direction of changes in EEG power spectra would be trending back towards the baseline values based on findings in [23]. To our knowledge, this is the first study investigating electrophysiological changes and correlation with clinical and biochemical measures in long term, i.e., during the 6-week treatment period and 4 weeks after.

The main part of this thesis firstly introduces the topic of the study including previous findings and states the hypotheses. The second chapter provides background information on MDD and suicidality, ketamine's uses and neurobiology, basics of EEG, and brief explanation of the biochemical measures used in the study. The third chapter explains the methodology used for the data acquisition and analysis, including a link to the project source code. The fourth chapter provides an overview of the findings (i.e., spectral changes of EEG between three timepoints and correlations with clinical and biochemical measures). The fifth chapter provides a discussion on the results and draws comparisons with previous findings.

2 Background

2.1 Major depressive disorder (MDD) and suicidality

MDD is a mental disorder that is characterised by depressed mood, diminished interests, impaired cognitive function, and vegetative symptoms (i.e., disturbed sleep or appetite). The disorder is diagnosed when one has at least one discrete depressive episode lasting at least 2 weeks according to DSM-5, which was released in 2013 [7].

MDD is directly linked with suicidal ideation and suicidal attempts, which can drastically reduce the quality of life of the person suffering from the disorder along with that of their family's [4]. People with MDD have an approximate 1.8-fold increase overall mortality and lose an estimated 10.6 and 7.2 life years for men and women, respectively [6]. Annually, approximately 800,000 deaths are attributed to suicide [27].

Presently, in treating MDD, there are two main options – psychotherapy and pharmacotherapy. Mild depressive episodes are usually treated with psychotherapy alone, but moderate-to-severe episodes combine the two therapies. Common psychotherapies used to treat MDD include cognitive-behavioural therapy, behavioural activation therapy, psychodynamic therapy, problem-solving therapy, interpersonal therapy, and mindfulness-based therapy. Accepted antidepressant drugs used within pharmacotherapy are serotonin reuptake inhibitors and serotonin-noradrenaline reuptake inhibitors, named after their pharmacological actions. However, it is estimated that other neurobiological systems could be involved in MDD as well, which are targeted by more experimental antidepressive agents, such as ketamine [4].

2.2 Ketamine

2.2.1 Clinical applications

Ketamine as treatment was initially introduced as an anaesthetic in 1964 and initially used on American soldiers during the Vietnam War. Currently, it is still a common anaesthetic

in paediatrics, field, and veterinary medicine due to its good safety profile. However, ketamine is also an addictive recreational drug and can result in physical harm (e.g., ulcerative cystitis), neurocognitive impairment, and deficits in working and episodic memory [28].

Historically, low dose (0.1-0.5 mg/kg) ketamine has been used for pain relief [29], in cases of prolonged epileptic seizures [30], and in MDD [31]. A review conducted in 2019 [32] suggests that intravenous low dose ketamine could be used to treat MDD, but its long-term effects need further studies. Similarly, low-dose ketamine for treatment of suicidality was reviewed in [24] and found compelling results to treat acute suicidal ideation, but long-term effectiveness of the drug needs to be further studied. Additionally, oral ketamine administration for depression was systematically reviewed in [33] due to its ease of use with the potential for high accessibility; significant antidepressant properties and good overall tolerability, but the effects were not as rapid as those associated with intravenous ketamine infusion.

2.2.2 Neurobiological mechanisms

Ketamine is a non-competitive NMDA receptor antagonist, meaning it blocks NMDA receptors binding glutamate predominantly. The resultant antidepressant effects are hypothesised to occur via two different pathways (Figure 1). Firstly, by direct blockage of NMDA receptors on postsynaptic glutamate neurons, levels of BDNF increase, and α -amino-3-hydroxy-5-methyl-4-isoxazolepropionic acid (AMPA) glutamate receptors get shuttled to the synapse, enhancing synaptic efficacy; all that due to not enabling the activation of eukaryotic elongation factor-2 (eEF2) from the blockage of NMDA receptor. Secondly, by indirectly blocking NMDA receptors on γ -aminobutyric acid (GABA) interneurons, inhibition of glutamate release in presynaptic glutamate neurons gets decreased, resulting in enhanced stimulation of AMPA receptors; thereby, creating a signalling cascade that raises BDNF levels. Release of BDNF results in the stimulation of tropomyosin receptor kinase B (TrkB) receptors which therefore activates the mammalian target of rapamycin complex 1 (mTORC1). Finally, local protein synthesis takes place increasing dendritic spine growth and restoring synaptic connectivity. Conclusively, these pathways and final changes are expected to be involved with antidepressant effects of ketamine [34], [35].

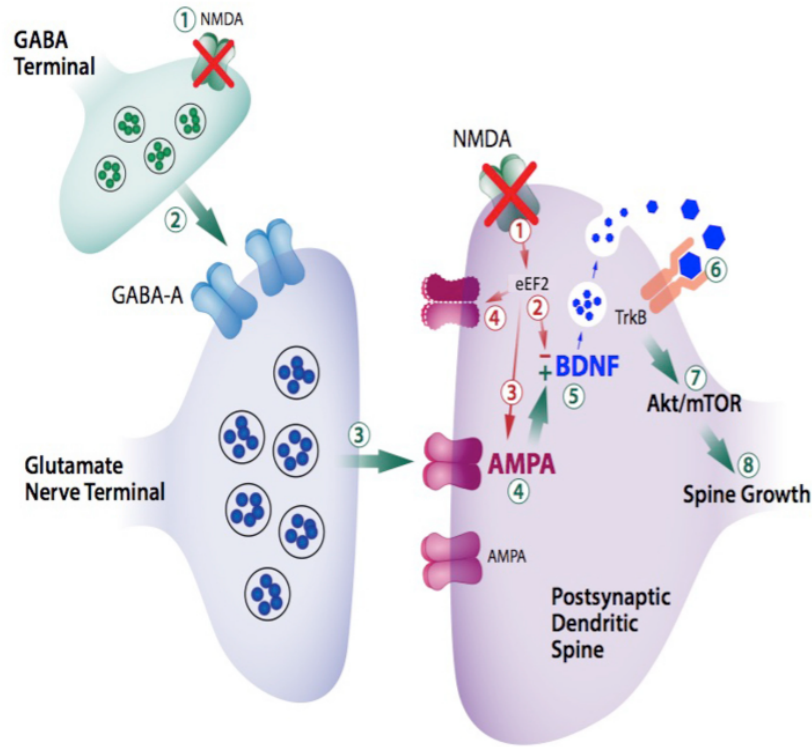


Figure 1. Antidepressant effects of ketamine are hypothesised to take place via two different pathways – by directly blocking NMDA receptors of postsynaptic glutamate neurons and/or blockade of NMDA receptors on GABA interneurons; both resulting in increased BDNF levels which increases dendritic spine growth and restores synaptic connectivity [34].

In addition to ketamine’s antidepressant effects, it also has anti-inflammatory and epigenetic effects which require further study. Furthermore, its efficacy may come from additional sites besides NMDA receptors. Also, ketamine’s isomers and metabolites differ in their mechanism of action and may have complementary or additive antidepressant effects [34], [36]. Other presumed antidepressants that increase glutamate release are serotonergic-based hallucinogens (e.g., LSD, psilocybin) which could serve as an entirely new class of antidepressant medications which could be the focus of MDD in future [34], [35], [37].

2.3 Electroencephalography

2.3.1 Neuronal activity

EEG is a non-invasive electrophysiology modality used to measure brain’s electric fields from the surface of the scalp (Figure 2). The measurement is done through a set of electrodes placed on the scalp of the subject. These electrodes record the difference of voltage potentials between the electrode and reference, which depend on the synchronous

electrical activity of underlying neuronal populations. However, because of its non-invasive nature, the neuronal signals reaching the electrodes get attenuated and distorted by volume conduction through various intracranial media and the scalp. Additionally, neuronal populations need to be active simultaneously (i.e., synchronous) for the voltage to be measurable at the scalp surface as this results in summation of currents that travel from the source to the electrodes [17].

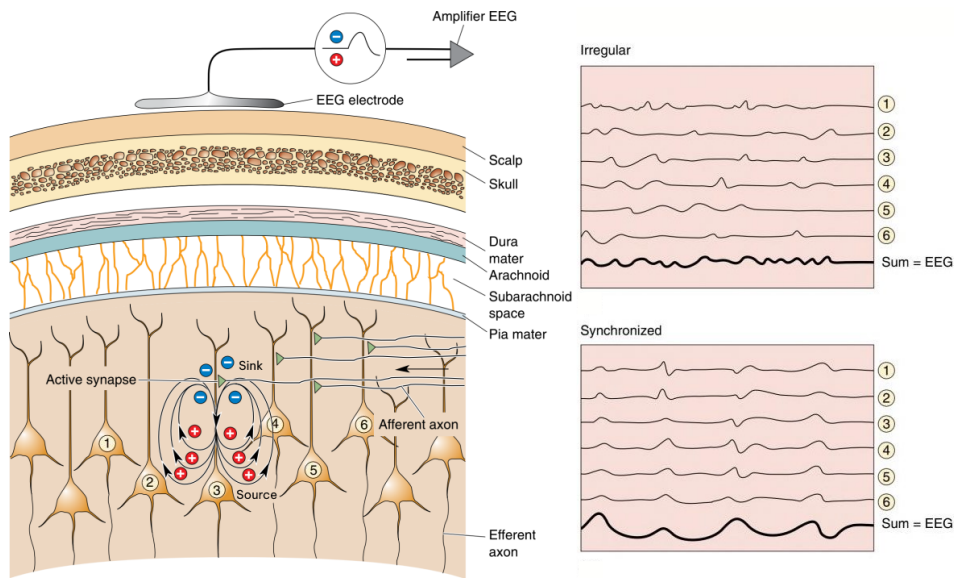


Figure 2. Fundamental logic of EEG measurement. The electrode approximates the signal from underlying neuronal population and their generated dipoles. The signal is the summation of the neurons' electrical activity – either irregular or synchronized. Figure adapted from [38].

More specifically, in case of excitatory activity, the postsynaptic neuron generates an extracellular voltage close to the neural dendrites that is more negative than elsewhere along the neuron. This region of negative charge is referred to as a 'sink' and positive charge 'source' – collectively called 'dipoles'. These neuronal current dipoles summed together from populations of neurons are measured by EEG electrodes. However, an electrode can only detect dipoles when it is closer to either the sink or the source side as otherwise the negative and positive sides will cancel each other out, resulting in net zero measurement [16].

2.3.2 Frequency domain analysis

EEG signals can be described by three main components – frequency, phase, and amplitude. The concept of analysing EEG waveforms based on their frequency components goes back to the inventor of the method. EEG was invented by a German psychiatrist Hans Berger (1873-1941) in 1924 when he used the new technique to record

the first human electroencephalogram. He later published an article “*Über das Elektrenkephalogramm des Menschen*” (“On the Human Electroencephalogram”), where he first characterised two types of brainwaves – alpha and beta [39].

In present day, the most common way to quantify EEG signals for psychiatric disorders functionally is by frequency bands – delta, theta, alpha, beta, and gamma (Figure 3; reviewed in [8]–[10]). This technique is called spectral analysis, frequency domain/band analysis, or band power analysis. Delta rhythms (<4 Hz) are prominent when the subject is in deep sleep [40], [41]. Theta rhythms (4-8 Hz) have been found to be related to emotional processing [42], [43] and are present when the subject is experiencing drowsiness [44]. Alpha rhythms (8-12 Hz) are inversely related to the electrical activity in the brain, meaning greater alpha band power reflects inactivity in the brain and vice versa [40]. This rhythm is best seen when the subject’s eyes are closed and during mental relaxation and is attenuated by opened eyes and mental effort [41], [44]. Beta rhythms (12-30 Hz) have been related to expectancy, anxiety, and introverted concentration [40], [45]. Gamma rhythms (>30 Hz) have been found to reflect attention and sensory systems [40] and mood swings [46].

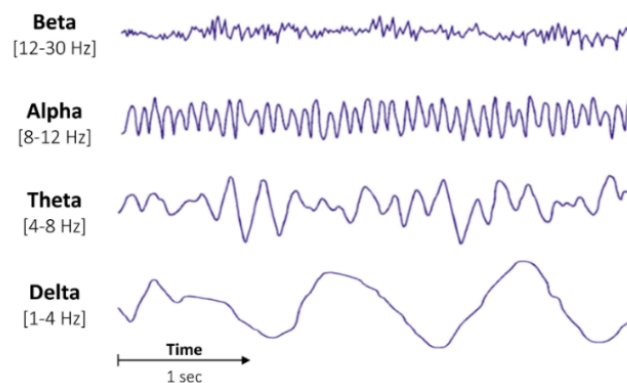


Figure 3. Commonly used predefined frequency bands and their EEG signals in time domain [47].

2.3.3 Signal artefacts and noise

When recording EEG, it is inevitable that the recorded signals include artefacts and noise from other sources besides neuronal activity in the brain (Figure 4). These sources can be environmental or biological. Some of the environmental artefacts are power line noise (around 50 or 60 Hz), electromagnetic fields (i.e., nearby cell phones), and mechanical vibrations (i.e., door slamming). Biological artefacts include physiological electrical

activity, such as cardiac, ocular, and muscular activity [17]. These artefacts are usually removed prior to analysis in a process referred to as signal pre-processing.

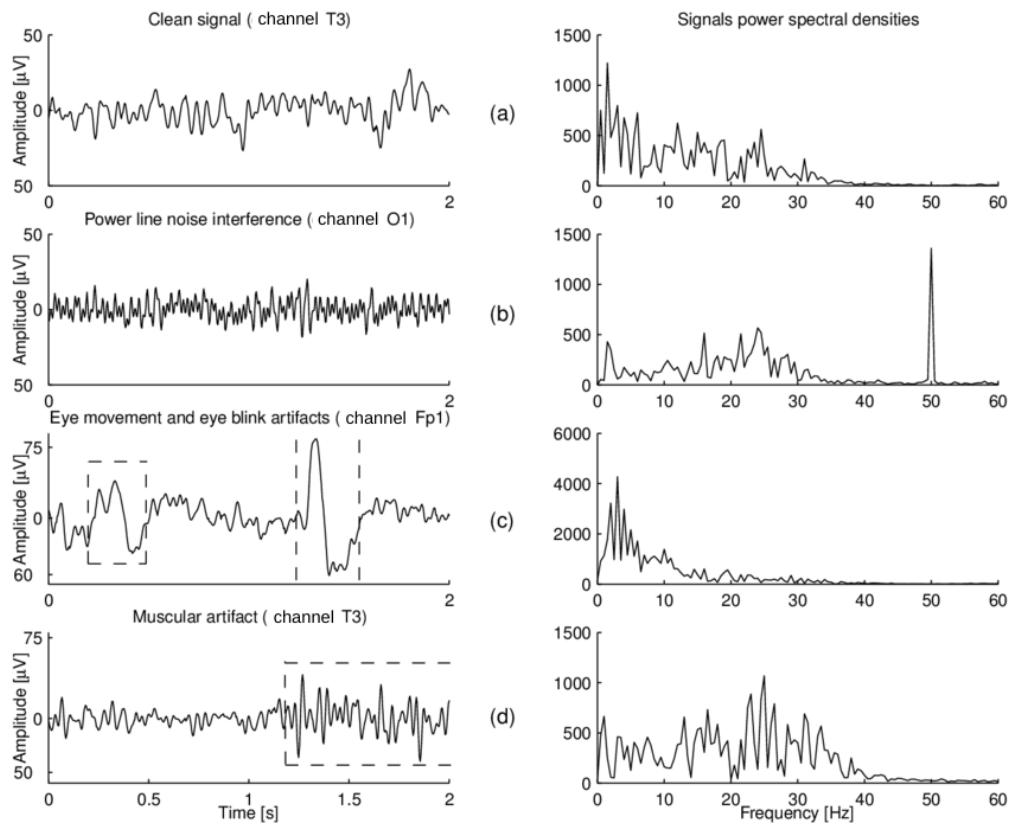


Figure 4. EEG signal artefacts and noise. Examples of these signals in time domain (left) and their corresponding power spectra in frequency domain (right) at various channel locations for (a) clean signal; (b) with power line noise; (c) with ocular artefacts; (d) with muscular artefacts [48].

2.4 Biochemistry

2.4.1 Brain-derived neurotrophic factor

BDNF is a neurotrophin that promotes the survival, growth, and maintenance of neurons in brain circuits involved in emotional and cognitive functions. More specifically, BDNF is synthesised as a precursor, pro-BDNF, which further transforms into mature BDNF which is then released into the extracellular space and processed [49]. Evidence suggests that abnormal levels of BDNF contributes to atrophy, synaptic disconnection, and dysfunction of brain circuits related to MDD [50]; in contrast, optimal levels of BDNF facilitate synaptic plasticity and remodelling, induction of long-term potentiation, modulation of gene expression for plasticity, resilience to neuronal insults, and alleviation of depressive symptoms [36], [51], [52].

Clinical studies have shown that the level and function of BDNF are altered in MDD patients. Reductions in mature BDNF in serum and plasma have been measured in people with depression [53], [54] and suicidality [55], [56]. A systematic review done in 2014 found significantly lower levels of serum mature and pro-BDNF in patients with unmedicated MDD compared to healthy controls [57]. On the other hand, the levels of BDNF seem to normalise with antidepressant and ketamine treatment [58].

2.4.2 Interleukin 6

IL-6 is a cytokine which is associated with an inflammatory response within the brain and several clinical studies have confirmed its role in stress and depression [59]. Additionally, it is thought that psychological stress is linked to elevated inflammation [60]. Regarding depression, IL-6 has been found to be elevated in patients with MDD compared to healthy controls according to three meta-analyses [61]–[63]. Furthermore, one clinical study found that the elevated IL-6 in a depressed population decreased at 4 hours after ketamine infusion, but then returned to baseline 24 h after infusion had ceased [64].

2.4.3 Endothelin 1

ET-1 is a peptide hormone responsible for various biological actions, including cardiovascular and neurological functions. Depression and cardiovascular morbidity and mortality are known to be related [65]. Supporting this, one previous study found that depression symptom severity predicted ET-1 elevation in patients with coronary artery disease [66].

3 Methodology

3.1 Study design

The whole project started with a pilot study which assessed safety, feasibility, and clinical outcomes of oral ketamine treatment [1]. This thesis is based on a follow-up study describing electrophysiological changes of the treatment [2] and its relationship with clinical outcomes and biochemical measures.

3.1.1 Clinical trial

An open-label clinical trial, Oral Ketamine Trial on Suicidality (OKTOS), was conducted at the Thompson Institute of University of the Sunshine Coast between August 2018 and November 2019 [1]. The intervention consisted of 6 weeks flexible-dose (0.5-3.0 mg/kg) treatment with oral ketamine and 4 weeks follow-up phase without the treatment. 30 participants received a total of six oral, sub-anaesthetic doses of ketamine for 6 weeks: one dose per week.

The trial had three major timepoints (Figure 5): (1) ‘baseline’ or ‘Pre’ (i.e., up to 2 weeks prior to treatment); (2) ‘post-treatment’, ‘Post’ or ‘6 weeks’ (i.e., 1-7 days after the final treatment); (3) ‘follow-up’, ‘FUP’ or ‘10 weeks’ (i.e., 28-32 days after the final treatment). The primary clinical outcome measure was reduction in suicidality with ketamine treatment and was determined by BSS. One of the secondary clinical measures was DASS, which is also included in this study.

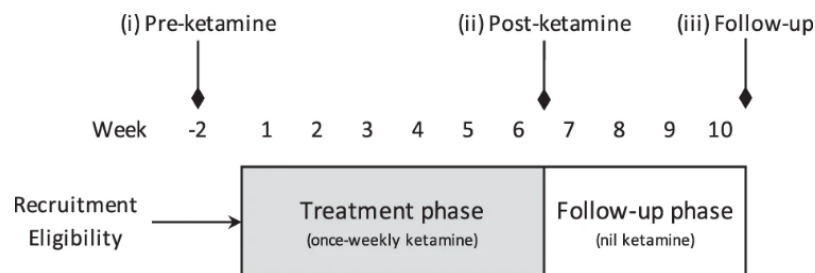


Figure 5. Clinical trial time schedule. Participants underwent treatment and follow-up phases, and three timepoints (i) baseline (‘Pre-ketamine’), (ii) post-treatment, and (iii) follow-up [1].

3.1.2 Participants

Of the total 32 participants who completed the trial, 25 were included in the analysis of EEG changes and correlations with clinical outcomes due to participant withdrawal (n=2 after 6 weeks) and missing electrophysiological recording session(s) (n=1 for Pre, n=1 for Post, n=3 for FUP). The final cohort of n= 25 participants included 11 males and 14 females who were aged from 22 to 71 years (mean = 46.41, standard deviation = 14.12). 20 participants out of these 25 were included in biochemical analysis due to missing datapoints for either BDNF, IL-6, or ET-1. These 20 participants included 10 males and 10 females who were aged from 22 to 71 years (mean = 47.45, standard deviation = 14.74).

All participants were clinically diagnosed with MDD and chronic suicidality (as per the DSM-5) and 76% had comorbid mental health conditions including generalised anxiety disorder (GAD), borderline personality disorder (BPD), post-traumatic stress disorder (PTSD), and/or substance use disorder (SUD). All but three subjects were reported ongoing use of psychotropic medications. See Table 2 in Appendix 2 for the full overview of the demographics, diagnosed disorders, and medications.

3.2 Data acquisition

3.2.1 Electrophysiological recordings

Participants were seated in a quiet, dimly lit room. Four minutes of eyes closed resting EEG data was acquired according to standard pharmaco-EEG procedures [67] with BioSemi ActiveTwo 32-channel system (Biosemi B.V, Amsterdam, Netherlands; Figure 6) at sampling rate of 1024 Hz. Scalp electrodes (Ag/AgCl active electrodes impedances < 40 k Ω) were localised according to the international 10/10 layout. Six additional electrodes were placed including left and right mastoids for reference and four electrooculographic (EOG) electrodes for obtaining horizontal and vertical eye movements.

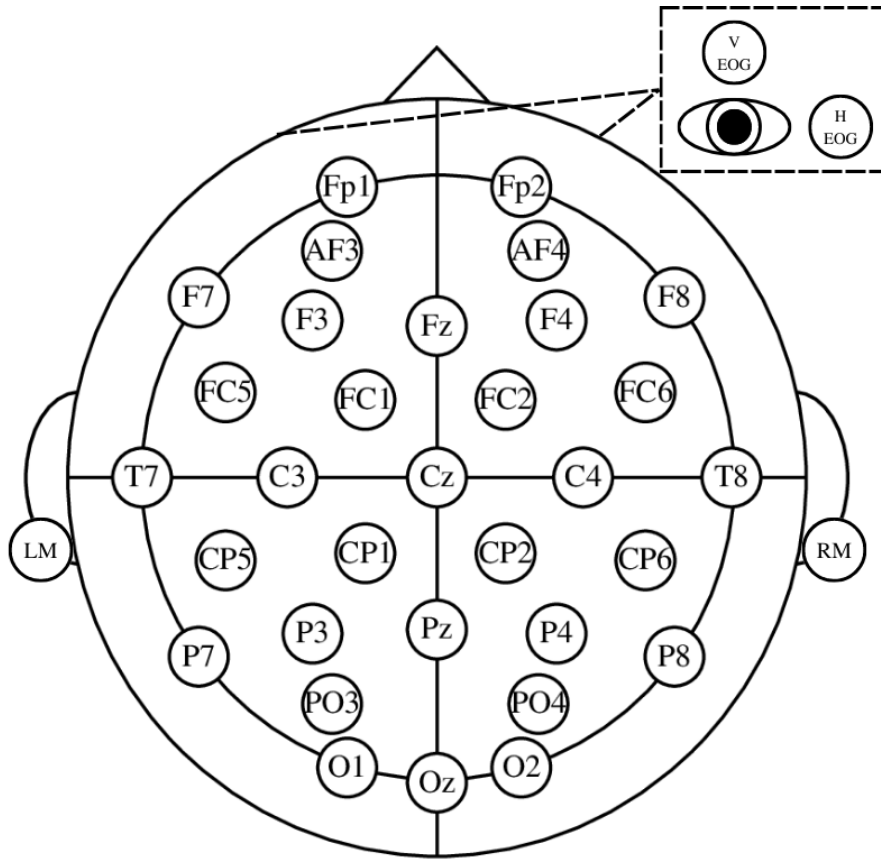


Figure 6. Electrode placement for BioSemi ActiveTwo 32-channel system with left and right mastoids, LM and RM, respectively, and horizontal and vertical EOG electrodes.

3.2.2 Blood testing

Peripheral blood samples were obtained from participants at all three timepoints. The plasma was extracted by centrifugating fresh blood samples with ethylenediaminetetraacetic acid as an anticoagulant and stored at -20°C until it was used for the study. Blood testing was always carried out in the morning to exclude any circadian or seasonal effect on BDNF, IL-6, or ET-1 concentrations. The concentrations were measured by the enzyme-linked immunoassay (ELISA) method.

3.3 Electroencephalographic analysis

An in-house EEG data processing pipeline ‘EEG-pyline’ was created and used for this study [3]. Using these scripts, acquired EEG signals were pre-processed, and spectral analysis was completed in brain regions of interest (Figure 11).

3.3.1 Signal pre-processing

All the signals were filtered with 0.5-30 Hz band-pass, finite impulse response (FIR), zero-phase, non-causal filter with Hamming window. In terms of filter characteristics, passband ripple and stopband attenuation depend on the chosen window in filter design. The chosen Hamming window provides up to 53 dB of stopband attenuation with relatively small 0.0194 dB passband ripple [68].

Required filter order was determined by the shortest transition bandwidth to ensure decent attenuation at the stop frequencies. Equation (1) displays the computation for filter order m , where C is a coefficient describing normalized transition width for a specific window type, Df is the shortest transition bandwidth, F_S is the sampling frequency [69].

$$m = \frac{C}{Df/F_S} \quad (1)$$

In this case, the shortest transition bandwidth was $Df = 0.5 \text{ Hz}$, coefficient for Hamming window $C = 3.3$, and sampling frequency $F_S = 1024 \text{ Hz}$. In result, the calculated filter order was $m = 6758$. Table 1 displays the filter parameters and Figure 7 illustrates the designed filter graphically.

Table 1. Filter parameters.

Parameter	Type/value used	Description/comments
Filter type	Band-pass, finite impulse response (FIR)	
Passband edges	0.5-30 Hz	Pre-defined frequency range of interest
Cut-off frequency	0.25 Hz; 33.75 Hz	As -6 dB cut-off
Filter order	6758	Based on Hamming window and the shortest transition bandwidth
Transition bandwidth	0.5 Hz (lower); 7.5 Hz (upper)	
Passband ripple	0.0194 dB	Based on Hamming window
Stopband attenuation	53 dB	Based on Hamming window
Filter delay	Zero-phase, non-causal	Delay is constant for all frequencies; zero phase distortion
Direction of computation	One-pass forward	

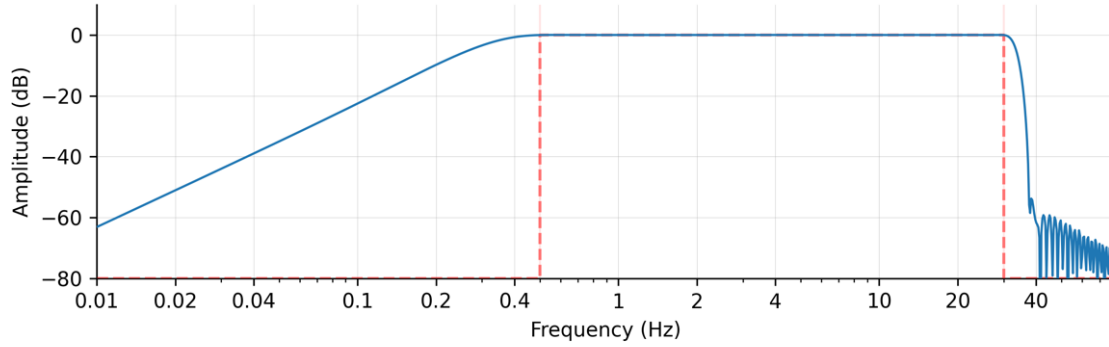


Figure 7. Amplitude response in frequency-domain of the designed filter (order 6758, zero-phase, band-pass, FIR). The graph displays the ideal filter (red dashed line) for 0.5-30 Hz band-pass but in reality, the transition bandwidths, passband ripples and stopband attenuation are never perfect.

EOG artefacts, including eye blinks and movements, were removed by computing signal-space projection [70] vectors using specific EOG channels acquired during EEG recording and applying these projections to the EEG signal to remove the artefacts. The previously mentioned steps were done using MNE package for Python [71].

Moreover, the signal was divided into equal-sized consecutive 5-second epochs without any overlap between epochs. Epochs were cleaned from artefacts in all channels using the Python package Autoreject (AR) (Figure 8) [72], [73]. This algorithm automates the EEG signal artefact rejection process, which is usually carried out via time-consuming manual visual inspection. The strategy of this algorithm is to estimate peak-to-peak thresholds for the signal amplitude for each channel using cross-validation (CV) with a robust error metric to remove or repair the artefactual epoch(s). AR has two methods for finding the threshold: global and local. Shortly, global AR finds one rejection threshold for all the channels and local AR goes through all channels separately and tries to repair artefactual epochs of a channel by interpreting from nearby channels, but if most of the channels for a given epoch are artefactual, the epoch is rejected.

In this study, both (global and local) AR procedures were applied. Firstly, global AR found a single threshold based on epochs in all channels and rejected epochs that exceeded this value. Secondly, local AR, with consensus level ($\kappa = 13$) and maximum channels to interpolate ($\rho = 4$), was run on all channels separately meaning when less than 13 channels were artefactual, a maximum of 4 channels were repaired, and if the before mentioned requirement was not satisfied, the whole epoch was rejected. The resulting EEG signals for each subject were screened visually using global field power plots to

check whether the magnitude of a signal is in similar scale throughout the whole signal meaning not having large artefacts in it (Figure 9).

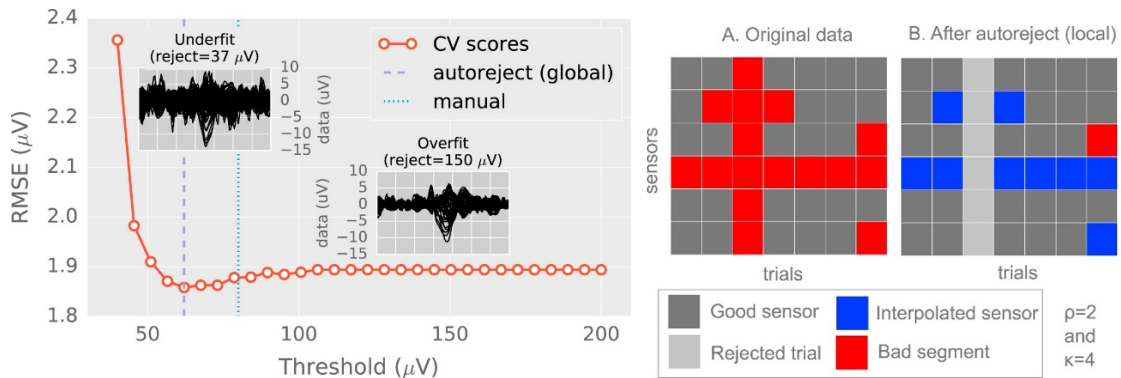


Figure 8. Artefact rejection process by Autoreject algorithm [73]. Left: global AR threshold estimation compared with manual human-set threshold where the used CV metric is the root mean squared error (RMSE) between the mean of the training set and the median of the validation set; for low threshold, the RMSE is high as most of the epochs are rejected (underfit) and for high threshold, the model does not drop any epochs (overfit); optimal threshold is in-between. Right: basis of local AR per each sensor (i.e., channel): the trial (i.e., epoch) is rejected if the number of bad channels $> \kappa$ and otherwise, the worst ρ sensors are interpolated (i.e., repaired).

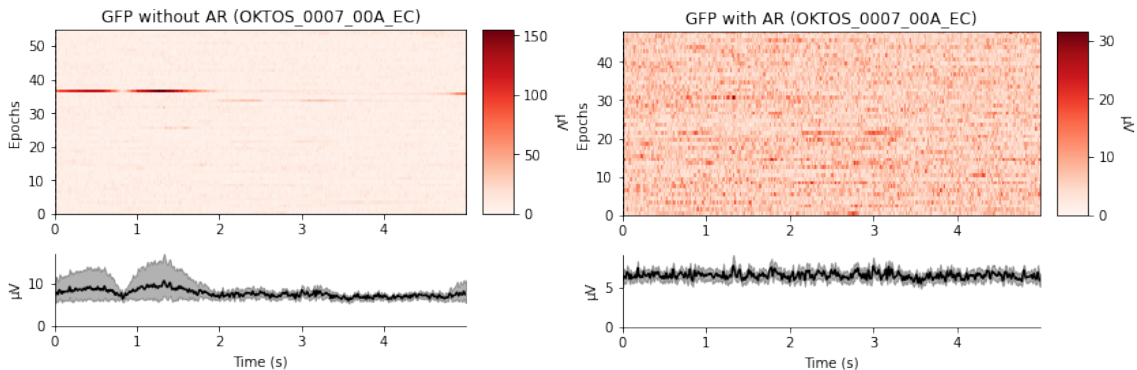


Figure 9. Global Field Power plots of one participant's EEG signals before (left) and after (right) artefact rejection.

3.3.2 Spectral analysis

The processed EEG signals were transformed into the frequency domain by estimating PSD using Welch's method [74], with 2-second Hamming window, 50% overlap. Average absolute power values ($\mu\text{V}^2/\text{Hz}$) were calculated for four frequency bands: delta (1-3.9 Hz), theta (4-7.9 Hz), alpha (8-12 Hz), low-beta (12.1-18 Hz), and high-beta (18.1-30 Hz). All 32 channels were averaged together into four brain regions: frontal (Fp1/2, AF3/4, F3/4, F7/8, Fz), temporal (FC5/6, T7/8, CP5/6, P7/8), centro-parietal (FC1/2, C3/4, Cz, CP1/2, P3/4, Pz), and occipital (PO3/4, O1/2, Oz).

Additionally, signal reliability was checked for each band by calculating z-scores using median (M) and median absolute deviation (MAD) [75] across all the epochs to determine if the PSD values fluctuated across time. As the participants were recorded in resting state, the power spectra were expected to not change more than two MADs across epochs. Each time the z-score was more than the before mentioned level, visual check was done by comparing first and second half of the signal topographically (Figure 10). If visual inspection confirmed that the given band was unreliable for multiple participants, the band was dropped. Delta band (1-3.9 Hz) values did not pass this reliability test within most of the subjects, thereby was not included in further analysis.

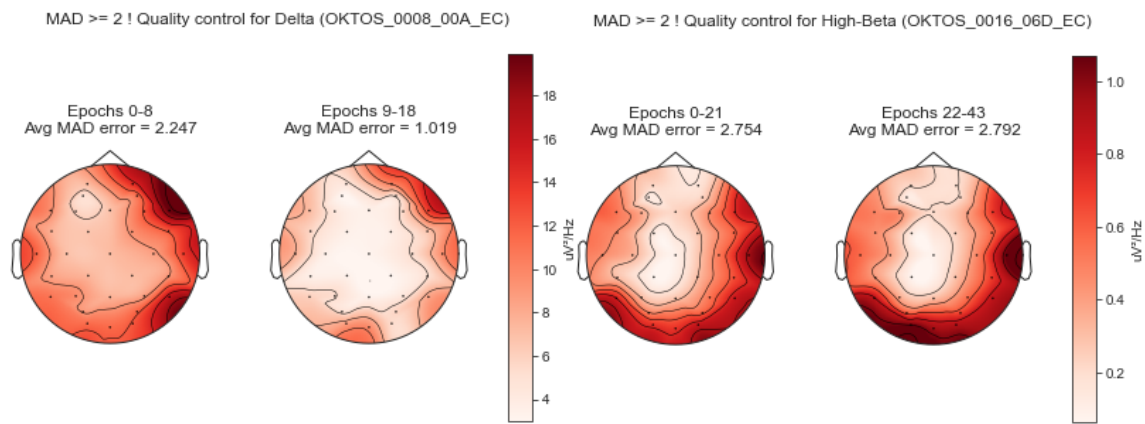


Figure 10. An example of the manual signal reliability check step via topographical plots. Two random cases where z-score $>$ 2 MAD and topographical plots for signal reliability were prompted to the analyst for visual check to make the final decision. The left plot shows clear power differences between the first and the second half of the EEG signal, thereby was marked 'bad delta' for the given participant. The right plot was allowed through to the analysis after the visual inspection.

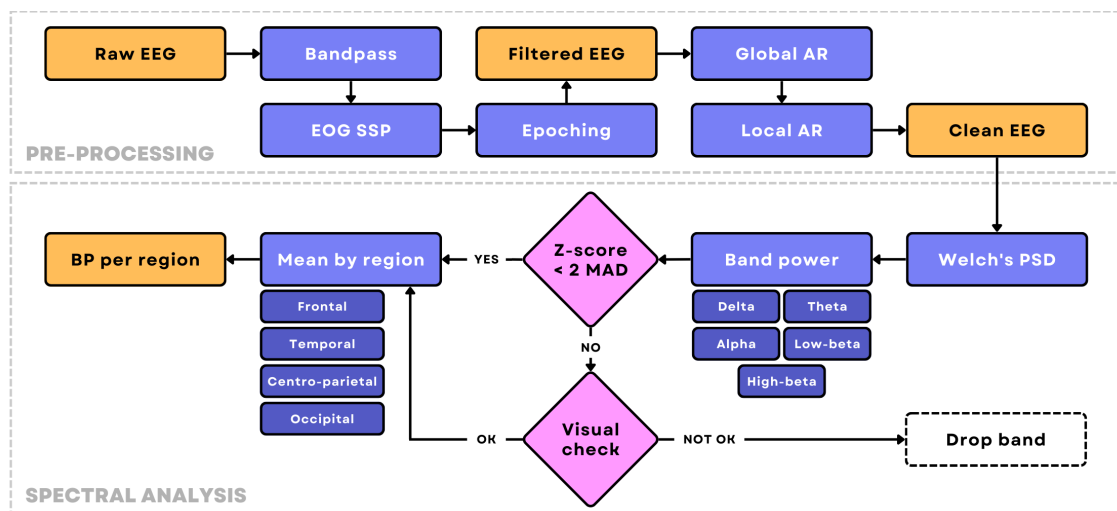


Figure 11. Flowchart of the EEG pipeline starting from pre-processing and ending with spectral analysis.

3.4 Correlation analysis

Correlation coefficients for changes between timepoints (i.e., baseline, post-treatment, and follow-up) were found for EEG power at all four frequency bands with biochemical results (BDNF, IL-6, ET-1) and two self-reported clinical measures (BSS, DASS). DASS includes three different measures which were used in the analysis separately: DASS-D for depression, DASS-A for anxiety, and DASS-S for stress. For calculating the coefficients, Spearman correlation was used due to the nature of non-gaussian distribution of the data [76]. Thresholds for the coefficients were set as the following: $\pm 0.3-0.5$ for low correlation; $\pm 0.5-0.7$ for moderate correlation; and $\pm 0.7-1.0$ for high correlation.

3.5 Statistics

To evaluate EEG power differences across different timepoints (i.e., baseline, post-treatment, and follow-up), a Wilcoxon signed-rank test was used. The non-parametric test was required since the EEG data did not meet the parametric assumptions (i.e., not normally distributed), and participants were compared to themselves across timepoints (i.e., paired samples). For statistical testing of the Spearman correlation coefficients, two-tailed t-test distributions were used. The significance threshold was set at $p < 0.05$. The statistical analysis and data visualisation were performed with the support of Pandas [77], [78], NumPy [79], SciPy [80], Matplotlib [81], [82], Seaborn [83] packages for Python. The EEG data is summarized and presented by measures of central tendency and dispersion – both by median (M) with interquartile range (IQR) and mean with standard deviation (SD) [84].

4 Results

4.1 Changes in band powers

4.1.1 Theta band

Theta band displayed significant changes only between post-treatment and follow-up timepoints. There were increases in power between post-treatment and follow-up timepoints at temporal ($M_{\text{Post}} = 2.641$, $IQR_{\text{Post}} = [1.194; 4.694] \rightarrow M_{\text{FUP}} = 2.784$, $IQR_{\text{FUP}} = [1.334; 5.932]$; $p_{\text{Post-FUP}} = 0.006$) and centro-parietal ($M_{\text{Post}} = 0.857$, $IQR_{\text{Post}} = [0.399; 1.492] \rightarrow M_{\text{FUP}} = 1.025$, $IQR_{\text{FUP}} = [0.437; 1.698]$; $p_{\text{Post-FUP}} = 0.019$) regions and a decrease in power for occipital region ($M_{\text{Post}} = 3.670$, $IQR_{\text{Post}} = [1.189; 5.140] \rightarrow M_{\text{FUP}} = 2.854$, $IQR_{\text{FUP}} = [1.375; 5.874]$; $p_{\text{Post-FUP}} = 0.012$) (Figure 12; Table 3).

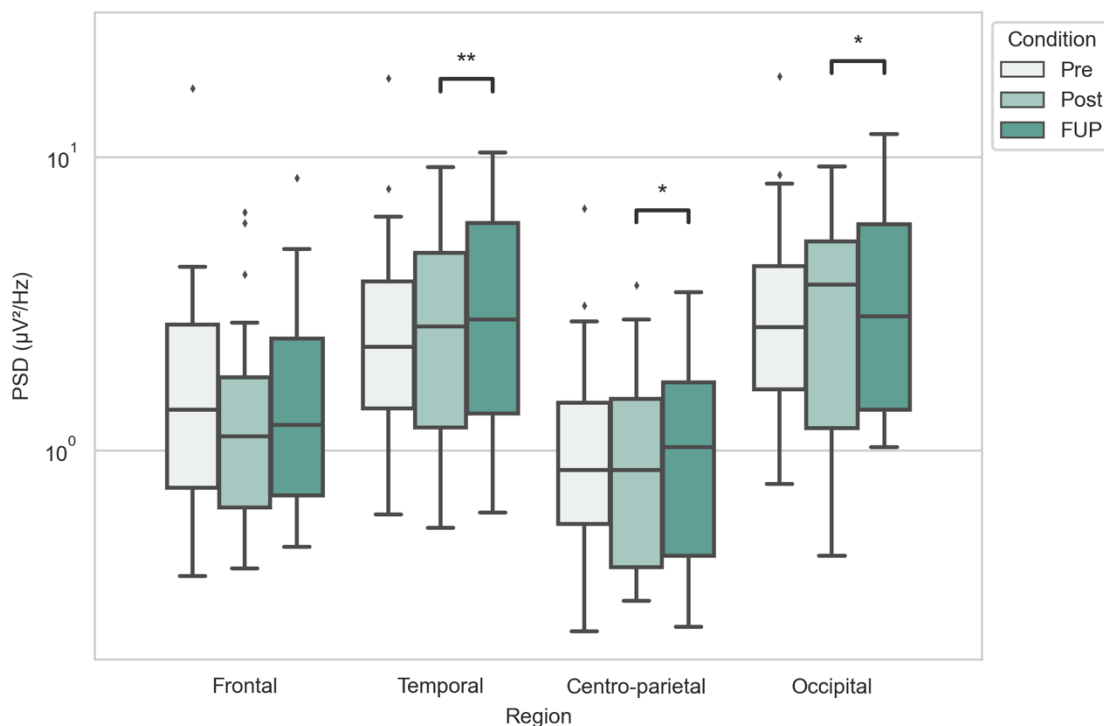


Figure 12. Theta band power for different timepoints and brain regions. Power spectra values have been plotted in a logarithmic scale y-axis. Statistical significance annotations are following: * $p < .05$; ** $p < .01$, and exact p-values can be found in Table 3.

4.1.2 Alpha band

Alpha band power at centro-parietal region was decreased between pre-treatment and post-treatment ($M_{Pre} = 2.248$, $IQR_{Pre} = [0.758; 3.605] \rightarrow M_{Post} = 1.635$, $IQR_{Post} = [0.871; 3.077]$; $p_{Pre-Post} = 0.048$), followed by an increase in power between post-treatment and follow-up timepoints ($M_{Post} = 1.635$, $IQR_{Post} = [0.871; 3.077] \rightarrow M_{FUP} = 2.004$, $IQR_{FUP} = [1.109; 3.574]$; $p_{Post-FUP} = 0.007$). Analyses similarly revealed an increase in power between post-treatment and follow-up timepoints at the temporal region ($M_{Post} = 3.989$, $IQR_{Post} = [2.263; 5.742] \rightarrow M_{FUP} = 4.130$, $IQR_{FUP} = [3.321; 8.034]$; $p_{Post-FUP} = 0.003$) (Figure 13; Table 4).

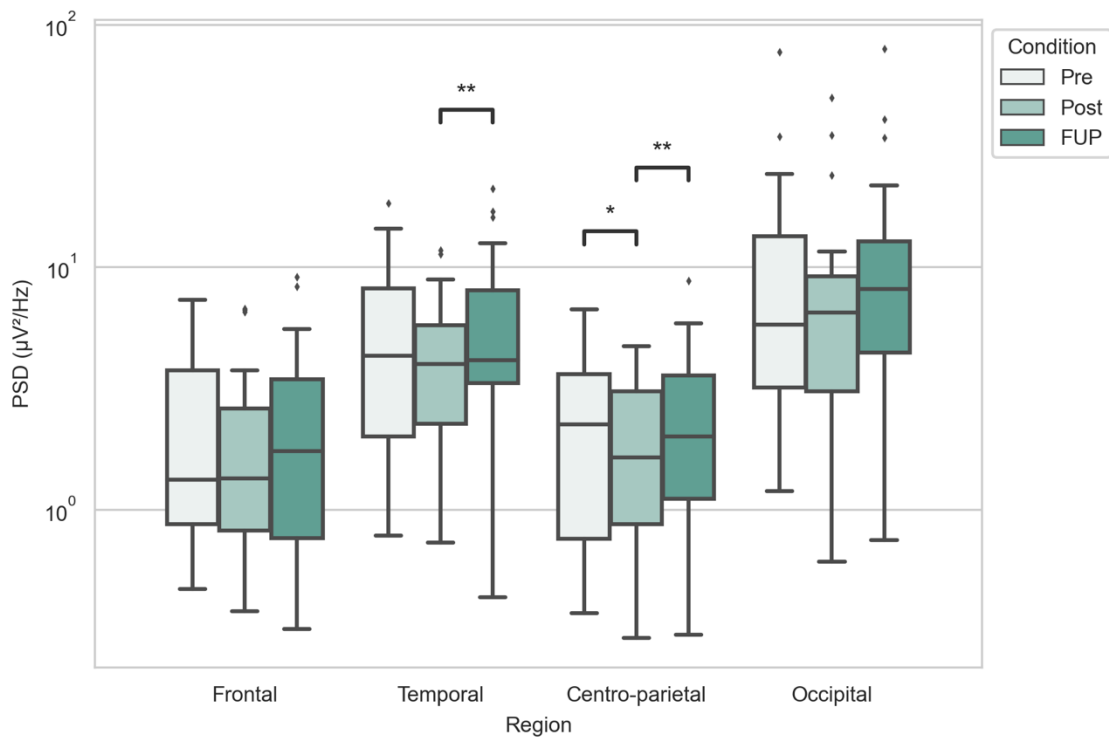


Figure 13. Alpha band power for different timepoints and brain regions. Power spectra values have been plotted in a logarithmic scale y-axis. Statistical significance annotations are following: * $p < .05$; ** $p < .01$, and exact p-values can be found in Table 4.

4.1.3 Low-beta band

Low-Beta band showed increase in power between post-treatment and follow-up timepoints at the occipital region ($M_{Post} = 0.987$, $IQR_{Post} = [0.708; 2.297] \rightarrow M_{FUP} = 1.170$, $IQR_{FUP} = [0.767; 2.224]$; $p_{Post-FUP} = 0.027$). Also, the power decreased between post-treatment and follow-up at temporal region ($M_{Post} = 1.042$, $IQR_{Post} = [0.701; 1.388] \rightarrow M_{FUP} = 0.953$, $IQR_{FUP} = [0.781; 1.665]$; $p_{Post-FUP} = 0.042$) (Figure 14; Table 5).

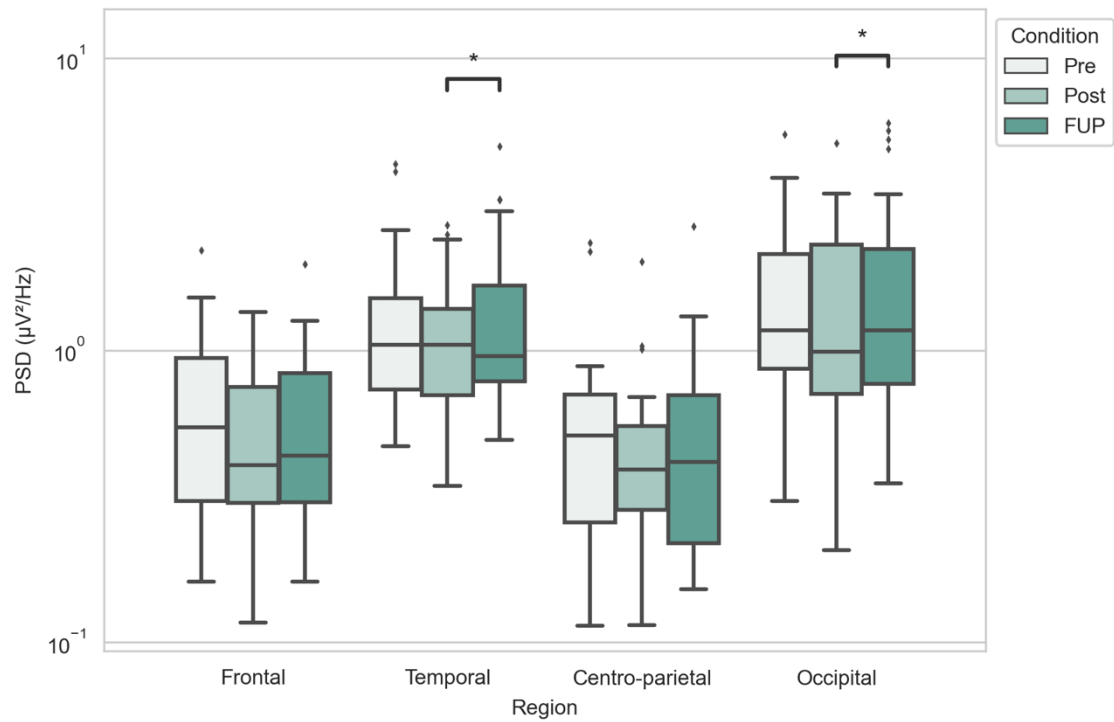


Figure 14. Low-beta band power for different timepoints and brain regions. Power spectra values have been plotted in a logarithmic scale y-axis. Statistical significance annotations are following: * $p < .05$, and exact p-values can be found in Table 5.

4.1.4 High-beta band

When comparing high-beta band power between pre-treatment-vs-post-treatment, post-treatment-vs-follow-up, or pre-treatment-vs-follow-up, no statistically significant differences were found (Figure 15; Table 6).

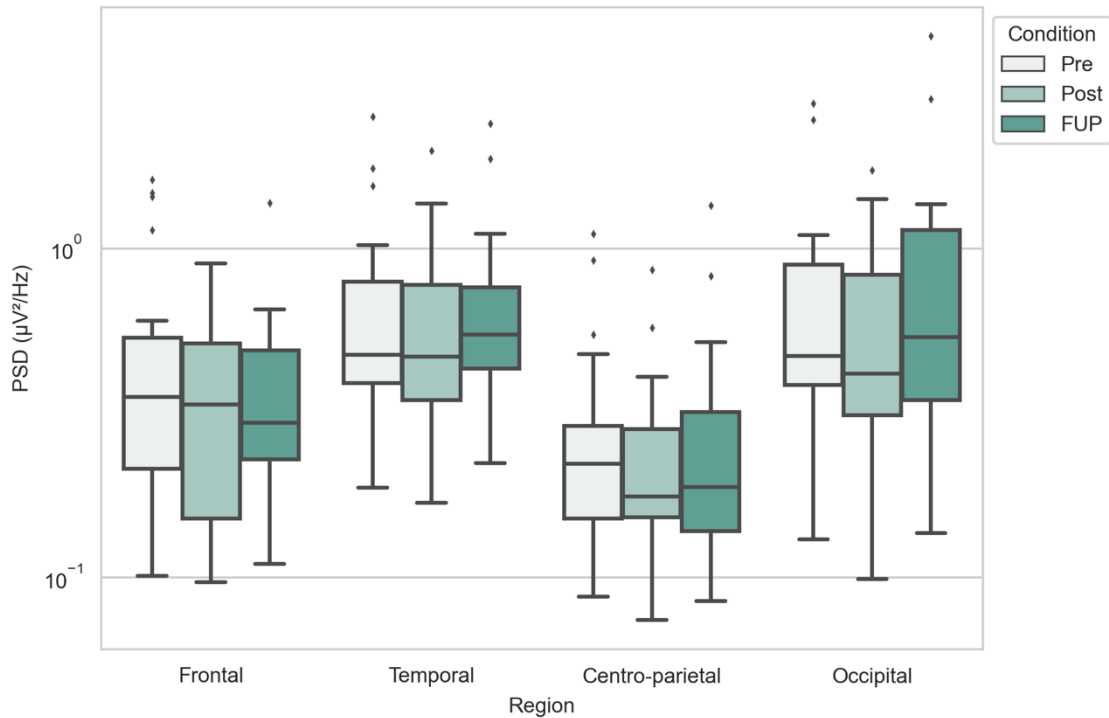


Figure 15. High-beta band power for different timepoints and brain regions. Power spectra values have been plotted in a logarithmic scale y-axis. Statistical significance levels can be found in Table 6.

4.2 Correlation with clinical outcomes

None of the power spectra changes within the four bands displayed any correlation with the main clinical outcome, BSS. However, the secondary clinical outcome measure, DASS, showed several significant correlations with the EEG spectral analysis results.

Change in DASS-D correlated with Post-FUP change in occipital theta ($r = 0.431$, $p = 0.032$; Figure 16); frontal low-beta ($r = -0.464$, $p = 0.019$); frontal high-beta ($r = -0.571$, $p = 0.003$), and with Pre-FUP change in occipital low-beta ($r = -0.421$, $p = 0.036$); temporal high-beta ($r = -0.504$, $p = 0.010$); and centro-parietal high-beta ($r = -0.420$, $p = 0.036$).

Change in DASS-A correlated with Pre-Post changes in occipital theta ($r = -0.522$, $p = 0.007$) and with Pre-FUP changes in centro-parietal theta ($r = -0.404$, $p = 0.045$); temporal alpha ($r = -0.455$, $p = 0.022$); and temporal high-beta ($r = -0.443$, $p = 0.027$).

Change in DASS-S correlated with Pre-Post changes in temporal theta ($r = -0.585$, $p = 0.002$); occipital low-beta ($r = -0.506$, $p = 0.010$); occipital theta ($r = -0.659$, $p = 0.0003$); temporal low-beta ($r = -0.528$, $p = 0.007$), and with Post-FUP changes in occipital theta

($r = 0.526$, $p = 0.007$, Figure 16), and with Pre-FUP changes in temporal alpha ($r = -0.402$, $p = 0.046$); temporal high-beta ($r = -0.595$, $p = 0.002$); and occipital high-beta ($r = -0.399$, $p = 0.048$). Tables 7-10 in Appendix 4 contain all mentioned correlation coefficients.

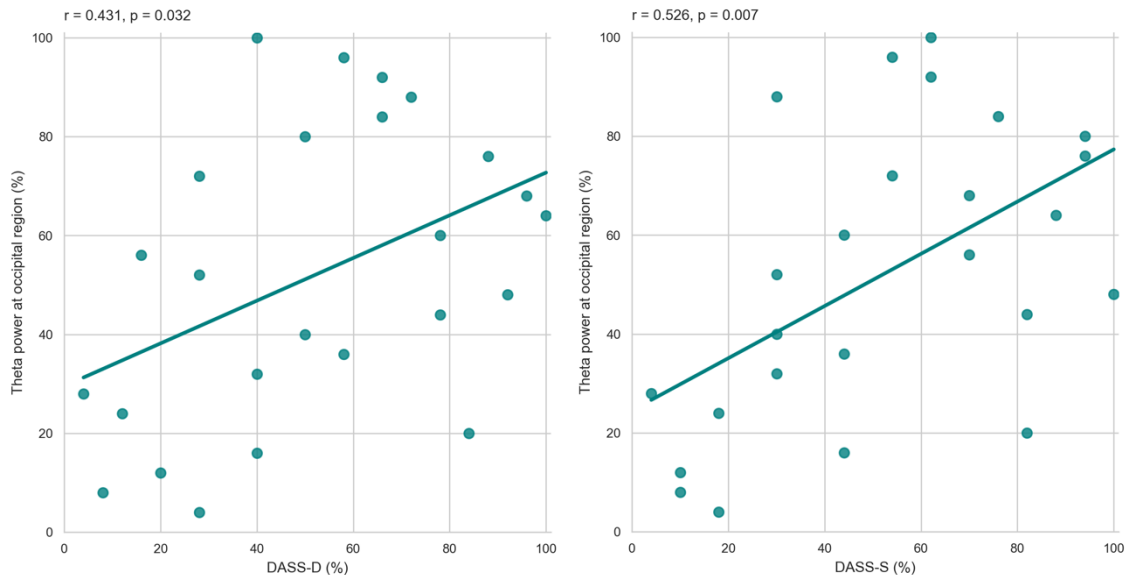


Figure 16. Theta at occipital region between post-treatment and follow-up timepoints (also had significant change in power, see Figure 12) correlates positively with DASS-D (left) and DASS-S (right). Displayed data is ranked and plotted in percentiles.

4.3 Correlation with biochemical measures

Power changes correlated with biochemical measures mostly between baseline and post-treatment timepoints in theta and alpha bands. Most correlated biochemical measure was IL-6 and least BDNF.

Change in BDNF correlated with Post-FUP change in centro-parietal theta ($r = -0.478$, $p = 0.033$, Figure 17) whereas the change of power between the timepoints was also statistically significant (Figure 12).

Change in IL-6 correlated with Pre-Post change in centro-parietal alpha ($r = 0.534$, $p = 0.015$, Figure 17) whereas the change of power between the timepoints was also statistically significant (Figure 13). Additionally, change in IL-6 correlated with Pre-Post change in frontal theta ($r = 0.519$, $p = 0.019$); temporal theta ($r = 0.496$, $p = 0.026$); centro-parietal theta ($r = 0.651$, $p = 0.002$); frontal alpha ($r = 0.568$, $p = 0.009$); frontal low-beta ($r = 0.677$, $p = 0.001$); temporal low-beta ($r = 0.481$, $p = 0.032$); centro-parietal low-beta

($r = 0.549$, $p = 0.012$); frontal high-beta ($r = 0.552$, $p = 0.012$); centro-parietal high-beta ($r = 0.537$, $p = 0.015$).

Change in ET-1 correlated with Pre-Post change in temporal theta ($r = 0.565$, $p = 0.009$) and occipital theta ($r = 0.477$, $p = 0.034$). Tables 11-14 in Appendix 5 contain all mentioned correlation coefficients.

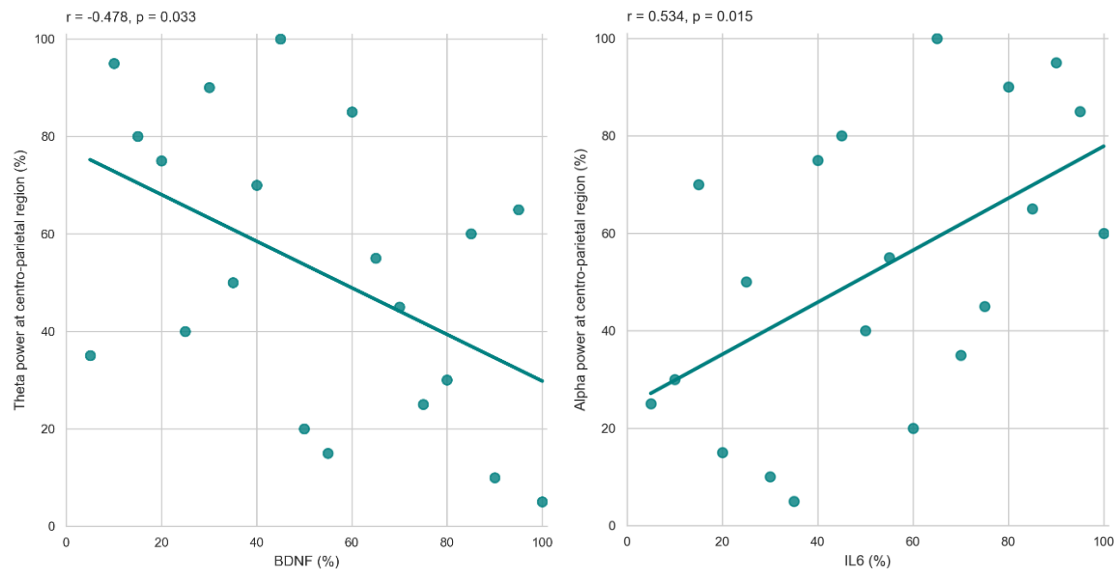


Figure 17. At centro-parietal region, theta between post-treatment and follow-up timepoints correlates negatively with BDNF (left) and alpha between baseline and post-treatment correlates positively with IL-6 (right). Both changes of band powers were also statistically significant (Figure 12, Figure 13). Displayed data is ranked and plotted in percentiles.

5 Discussion

The main objective of this study was to explore spectral changes of EEG in patients with MDD and chronic suicidality following 6 weeks of low-dose oral ketamine treatment. Secondly, it was to investigate correlations between changes in EEG spectral results and changes in clinical and biochemical measures.

The most conclusive finding was the hypothesized alpha band power change at the centro-parietal region. Between baseline and post-treatment timepoints, the power decreased and after the treatment period (i.e., between post-treatment and follow-up) it increased again at centro-parietal region (Figure 13, Figure 18). Similar changes were also reported in another recent study including ketamine as treatment for depression [23]. Similarly, we found alpha band power significantly increasing between the post-treatment and follow-up timepoints at temporal region. However, at that same region a decrease in power before, between baseline and post-treatment, was not statistically significant. As alpha band power has been found to be higher in depressive subjects compared to healthy controls [18], [19], our findings suggest that low-dose oral ketamine decreases alpha band power at centro-parietal region, but the changes revert close to pre-treatment levels after ketamine treatment has ceased. We did not find any statistically significant change between alpha band power between pre-treatment and follow-up (Figure 13), which suggests the effects of ketamine are transient in terms of changes in alpha activity.

For theta band, we did not find any power changes immediately following the treatment period (i.e., week 6), but there were significant changes between post-treatment and follow-up timepoints – power was decreased at the occipital region and increased at temporal and centro-parietal regions (Figure 12, Figure 18). Similar to our results, another study reported an increase in theta band power after some period of time had passed after stopping the treatment [23]. However, in our case, the follow-up was 4 weeks, and in their study, it was after 2 hours, so the results are not directly comparable. Other clinical studies (which did not include ketamine treatment) have found theta power to be higher in participants with depression compared to healthy controls. For example, theta power has

been found to be increased at parietal and occipital regions [18] and frontal and central regions [20]. Based on these studies, the occipital theta decrease observed here could represent a delayed positive treatment effect due to ketamine-induced neuroplastic changes. In contrast, an increase in temporal and centro-parietal theta power would suggest the opposite – that treatment effects have ceased, and the depressive pathophysiology returns. Thereby, theta band power changes in our study are inconclusive, and more studies are needed to confirm the function of theta band power in depression and suicidality, and whether this is ameliorated by ketamine treatment.

High-beta band showed no significant power changes across timepoints (Figure 15), but low-beta power between post-treatment and follow-up decreased at temporal region and increased at occipital region (Figure 14, Figure 18). Our findings for beta bands were not consistent with previous findings [23]. In terms of cognitive functions, a recent study found that low-beta (and alpha) band powers at parieto-occipital region reflect one’s sense of agency [85], whereas distorted sense of agency has been suggested to be linked to several neuropsychiatric disorders including depression [86]. Beta band activity has also been related to anxiety previously [40], [45], which itself has been used to predict suicidal ideation [87]; indicating an indirect relationship. Therefore, ketamine’s therapeutic effect on depression and suicidality reported here could be mediated by changes in beta band activity that influence sense of agency and/or symptoms of anxiety, but further studies are needed for more precise conclusions.

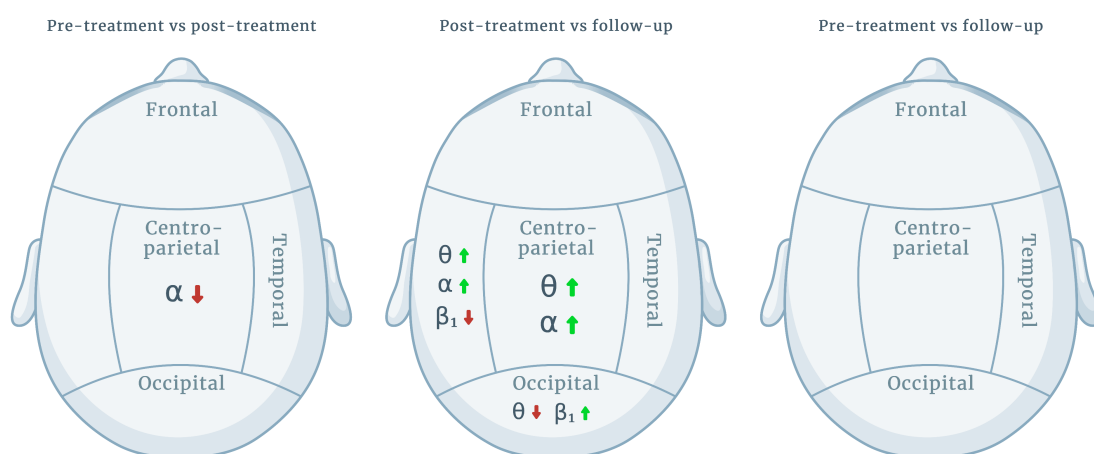


Figure 18. Illustrative visualisation of brain regions and significant changes in band powers between baseline and post-treatment (left), between post-treatment and follow-up (middle), and between pre-treatment and follow-up timepoints. Created with BioRender.com.

Whilst none of the power spectra changes correlated with the main clinical outcome (BSS), several significant relationships with the secondary measure (DASS) were found. One of the most relevant correlation findings was the theta band power change at occipital region showed a moderate positive correlation with DASS-S and weak positive correlation with DASS-D between post-treatment and follow-up timepoints (Figure 16). This is relevant because the changes at occipital region for theta band power between post-treatment and follow-up were also statistically significant (Figure 12).

Correlation with biochemical measures emerged mostly during the treatment (i.e., between baseline and post-treatment) in the case of IL-6 and ET-1. One of the notable correlations between IL-6 was positive correlation with alpha band change during the treatment period at centro-parietal region (Figure 17) whereas that band power change was also statistically significant (Figure 18). BDNF displayed less correlation with EEG band power changes, but its changes correlated mostly after the treatment had ended. Between post-treatment and follow-up timepoints, theta band power change at centro-parietal region correlated negatively with BDNF (Figure 17) whereas the power change was also statistically significant (Figure 12).

In this study, there were several limitations which may have impacted the results. Firstly, the sample size was relatively small, which may have impacted the results. Secondly, the neurological effects of concurrent medications could not be excluded as most of the participants were taking various psychotropic medications throughout the trial. Finally, this study focused on chronic suicidality (i.e., patients with suicidality for at least six months), and there may be different outcomes if this period of duration changes.

This study found that long-term low-dose oral ketamine treatment resulted in significant changes in EEG power spectra in adults with MDD and chronic suicidality. However, further studies of low-dose oral ketamine in suicidality are needed using a randomised control study design and larger sample size to address the limitations of the current open-label trial.

6 Summary

The main aim of this thesis was to investigate electrophysiological changes during and after 6-week low-dose oral ketamine treatment in depressive and suicidal adults. It was found that ketamine treatment decreased alpha band power during the active treatment phase, but these changes returned towards the baseline after the treatment ceased – suggesting ketamine’s effects are transient. However, multiple other power changes in theta, alpha, and low-beta bands occurred after the treatment had stopped which could be explained by delayed ketamine-induced neuroplastic changes. Some of the changes in band power between time points were associated with DASS, but not with BSS. BDNF had a correlation with the changes in band power after the treatment phase, while IL-6 and ET-1 showed correlations during treatment.

In addition to studying the effects of ketamine, the EEG pipeline used in this analysis was proposed and created with an aim to make signal pre-processing semi-automated and less time-consuming using the most recent reliable methods and tools. There are software solutions which handle most of the signal processing and analysis automatically, but they are expensive and use a so-called “black-box” approach, meaning it is often hard to know what the code is actually “doing”.

References

- [1] A. T. Can *et al.*, “Low dose oral ketamine treatment in chronic suicidality: An open-label pilot study,” *Transl. Psychiatry*, vol. 11, no. 1, Art. no. 1, Feb. 2021, doi: 10.1038/s41398-021-01230-z.
- [2] T. E. Anijärv *et al.*, “Spectral changes of EEG following a 6-week low-dose oral ketamine treatment in adults with major depressive disorder and chronic suicidality,” *Int. J. Neuropsychopharmacol.*, p. pyad006, Feb. 2023, doi: 10.1093/ijnp/pyad006.
- [3] T. E. Anijärv, “EEG-pyline: EEG pipeline in Python.” Zenodo, Dec. 16, 2022. Accessed: Dec. 21, 2022. [Online]. Available: <https://doi.org/10.5281/zenodo.7444821>
- [4] C. Otte *et al.*, “Major depressive disorder,” *Nat. Rev. Dis. Primer*, vol. 2, no. 1, Art. no. 1, Sep. 2016, doi: 10.1038/nrdp.2016.65.
- [5] World Health Organization, “Suicide prevention,” *World Health Organization*, 2021. <https://www.who.int/health-topics/suicide>
- [6] E. Chesney, G. M. Goodwin, and S. Fazel, “Risks of all-cause and suicide mortality in mental disorders: a meta-review,” *World Psychiatry*, vol. 13, no. 2, pp. 153–160, Jun. 2014, doi: 10.1002/wps.20128.
- [7] American Psychiatric Association and American Psychiatric Association, Eds., *Diagnostic and statistical manual of mental disorders: DSM-5*, 5th ed. Washington, D.C: American Psychiatric Association, 2013.
- [8] F. S. de Aguiar Neto and J. L. G. Rosa, “Depression biomarkers using non-invasive EEG: A review,” *Neurosci. Biobehav. Rev.*, vol. 105, pp. 83–93, Oct. 2019, doi: 10.1016/j.neubiorev.2019.07.021.
- [9] A. Dev *et al.*, “Exploration of EEG-Based Depression Biomarkers Identification Techniques and Their Applications: A Systematic Review,” *IEEE Access*, vol. 10, pp. 16756–16781, 2022, doi: 10.1109/ACCESS.2022.3146711.
- [10] J. J. Newson and T. C. Thiagarajan, “EEG Frequency Bands in Psychiatric Disorders: A Review of Resting State Studies,” *Front. Hum. Neurosci.*, vol. 12, p. 521, Jan. 2019, doi: 10.3389/fnhum.2018.00521.
- [11] T. Wise, A. J. Cleare, A. Herane, A. H. Young, and D. Arnone, “Diagnostic and therapeutic utility of neuroimaging in depression: an overview,” *Neuropsychiatr. Dis. Treat.*, vol. 10, pp. 1509–1522, Aug. 2014, doi: 10.2147/NDT.S50156.
- [12] K. Sudol and J. J. Mann, “Biomarkers of Suicide Attempt Behavior: Towards a Biological Model of Risk,” *Curr. Psychiatry Rep.*, vol. 19, no. 6, p. 31, May 2017, doi: 10.1007/s11920-017-0781-y.
- [13] W. Liao, J. Li, X. Duan, Q. Cui, H. Chen, and H. Chen, “Static and dynamic connectomics differentiate between depressed patients with and without suicidal ideation,” *Hum. Brain Mapp.*, vol. 39, no. 10, pp. 4105–4118, 2018, doi: 10.1002/hbm.24235.
- [14] A. N. Goldstein-Piekarski *et al.*, “Mapping Neural Circuit Biotypes to Symptoms and Behavioral Dimensions of Depression and Anxiety,” *Biol. Psychiatry*, vol. 91, no. 6, pp. 561–571, Mar. 2022, doi: 10.1016/j.biopsych.2021.06.024.

- [15] V. S. Sohal and J. L. R. Rubenstein, “Excitation-inhibition balance as a framework for investigating mechanisms in neuropsychiatric disorders,” *Mol. Psychiatry*, vol. 24, no. 9, Art. no. 9, Sep. 2019, doi: 10.1038/s41380-019-0426-0.
- [16] A. F. Jackson and D. J. Bolger, “The neurophysiological bases of EEG and EEG measurement: A review for the rest of us,” *Psychophysiology*, vol. 51, no. 11, pp. 1061–1071, 2014, doi: 10.1111/psyp.12283.
- [17] A. Biasucci, B. Franceschiello, and M. M. Murray, “Electroencephalography,” *Curr. Biol.*, vol. 29, no. 3, pp. R80–R85, Feb. 2019, doi: 10.1016/j.cub.2018.11.052.
- [18] V. A. Grin-Yatsenko, I. Baas, V. A. Ponomarev, and J. D. Kropotov, “Independent component approach to the analysis of EEG recordings at early stages of depressive disorders,” *Clin. Neurophysiol.*, vol. 121, no. 3, pp. 281–289, Mar. 2010, doi: 10.1016/j.clinph.2009.11.015.
- [19] N. Jaworska, P. Blier, W. Fusee, and V. Knott, “Alpha power, alpha asymmetry and anterior cingulate cortex activity in depressed males and females,” *J. Psychiatr. Res.*, vol. 46, no. 11, pp. 1483–1491, Nov. 2012, doi: 10.1016/j.jpsychires.2012.08.003.
- [20] S. M. Lee, K.-I. Jang, and J.-H. Chae, “Electroencephalographic Correlates of Suicidal Ideation in the Theta Band,” *Clin. EEG Neurosci.*, vol. 48, no. 5, pp. 316–321, Sep. 2017, doi: 10.1177/1550059417692083.
- [21] M. Bachmann *et al.*, “Methods for classifying depression in single channel EEG using linear and nonlinear signal analysis,” *Comput. Methods Programs Biomed.*, vol. 155, pp. 11–17, Mar. 2018, doi: 10.1016/j.cmpb.2017.11.023.
- [22] Z. Cao, C.-T. Lin, W. Ding, M.-H. Chen, C.-T. Li, and T.-P. Su, “Identifying Ketamine Responses in Treatment-Resistant Depression Using a Wearable Forehead EEG,” *IEEE Trans. Biomed. Eng.*, vol. 66, no. 6, pp. 1668–1679, Jun. 2019, doi: 10.1109/TBME.2018.2877651.
- [23] S. de la Salle, J. L. Phillips, P. Blier, and V. Knott, “Electrophysiological correlates and predictors of the antidepressant response to repeated ketamine infusions in treatment-resistant depression,” *Prog. Neuropsychopharmacol. Biol. Psychiatry*, vol. 115, p. 110507, Apr. 2022, doi: 10.1016/j.pnpbp.2021.110507.
- [24] F. Mallick and C. B. McCullumsmith, “Ketamine for Treatment of Suicidal Ideation and Reduction of Risk for Suicidal Behavior,” *Curr. Psychiatry Rep.*, vol. 18, no. 6, p. 61, May 2016, doi: 10.1007/s11920-016-0680-7.
- [25] R. Shinohara, G. K. Aghajanian, and C. G. Abdallah, “Neurobiology of the Rapid-Acting Antidepressant Effects of Ketamine: Impact and Opportunities,” *Biol. Psychiatry*, vol. 90, no. 2, pp. 85–95, Jul. 2021, doi: 10.1016/j.biopsych.2020.12.006.
- [26] J. J. Wong, O. O’Daly, M. A. Mehta, A. H. Young, and J. M. Stone, “Ketamine modulates subgenual cingulate connectivity with the memory-related neural circuit—a mechanism of relevance to resistant depression?,” *PeerJ*, vol. 4, p. e1710, Feb. 2016, doi: 10.7717/peerj.1710.
- [27] B. Harmer, S. Lee, T. vi H. Duong, and A. Saadabadi, “Suicidal Ideation,” in *StatPearls*, Treasure Island (FL): StatPearls Publishing, 2022. Accessed: Aug. 02, 2022. [Online]. Available: <http://www.ncbi.nlm.nih.gov/books/NBK565877/>
- [28] C. J. A. Morgan, H. V. Curran, and the I. S. C. on Drugs (ISCD), “Ketamine use: a review,” *Addiction*, vol. 107, no. 1, pp. 27–38, 2012, doi: 10.1111/j.1360-0443.2011.03576.x.
- [29] G. E. Correll, J. Maleki, E. J. Gracely, J. J. Muir, and R. E. Harbut, “Subanesthetic Ketamine Infusion Therapy: A Retrospective Analysis of a Novel

- Therapeutic Approach to Complex Regional Pain Syndrome,” *Pain Med.*, vol. 5, no. 3, pp. 263–275, Sep. 2004, doi: 10.1111/j.1526-4637.2004.04043.x.
- [30] D. G. Fujikawa, “Neuroprotective Effect of Ketamine Administered After Status Epilepticus Onset,” *Epilepsia*, vol. 36, no. 2, pp. 186–195, 1995, doi: 10.1111/j.1528-1157.1995.tb00979.x.
- [31] R. M. Berman *et al.*, “Antidepressant effects of ketamine in depressed patients,” *Biol. Psychiatry*, vol. 47, no. 4, pp. 351–354, Feb. 2000, doi: 10.1016/S0006-3223(99)00230-9.
- [32] A. Corrigan and G. Pickering, “Ketamine and depression: a narrative review,” *Drug Des. Devel. Ther.*, vol. 13, pp. 3051–3067, Aug. 2019, doi: 10.2147/DDDT.S221437.
- [33] J. D. Rosenblat, A. F. Carvalho, M. Li, Y. Lee, M. Subramanieapillai, and R. S. McIntyre, “Oral Ketamine for Depression: A Systematic Review,” *J. Clin. Psychiatry*, vol. 80, no. 3, p. 13514, Apr. 2019, doi: 10.4088/JCP.18r12475.
- [34] J. H. Krystal, C. G. Abdallah, G. Sanacora, D. S. Charney, and R. S. Duman, “Ketamine: A Paradigm Shift for Depression Research and Treatment,” *Neuron*, vol. 101, no. 5, pp. 774–778, Mar. 2019, doi: 10.1016/j.neuron.2019.02.005.
- [35] C. Driver, T. N. W. Jackson, J. Lagopoulos, and D. F. Hermens, “Molecular mechanisms underlying the N-methyl-d-aspartate receptor antagonists: Highlighting their potential for transdiagnostic therapeutics,” *Prog. Neuropsychopharmacol. Biol. Psychiatry*, vol. 119, p. 110609, Dec. 2022, doi: 10.1016/j.pnpbp.2022.110609.
- [36] R. S. Duman, G. K. Aghajanian, G. Sanacora, and J. H. Krystal, “Synaptic plasticity and depression: new insights from stress and rapid-acting antidepressants,” *Nat. Med.*, vol. 22, no. 3, Art. no. 3, Mar. 2016, doi: 10.1038/nm.4050.
- [37] D. D. Gregorio *et al.*, “Hallucinogens in Mental Health: Preclinical and Clinical Studies on LSD, Psilocybin, MDMA, and Ketamine,” *J. Neurosci.*, vol. 41, no. 5, pp. 891–900, Feb. 2021, doi: 10.1523/JNEUROSCI.1659-20.2020.
- [38] M. F. Bear, B. W. Connors, and M. A. Paradiso, *Neuroscience: exploring the brain*, Enhanced fourth edition. Burlington, MA: Jones & Bartlett Learning, 2016.
- [39] H. Berger, “Über das Elektrenkephalogramm des Menschen,” *Arch. Für Psychiatr. Nervenkrankh.*, vol. 94, no. 1, pp. 16–60, Dec. 1931, doi: 10.1007/BF01835097.
- [40] W. J. Freeman and R. Quian Quiroga, *Imaging brain function with EEG: advanced temporal and spatial analysis of electroencephalographic signals*. New York: Springer, 2013.
- [41] Nilesh. N. Kulkarni and V. K. Bairagi, “Electroencephalogram based diagnosis of Alzheimer Disease,” in *2015 IEEE 9th International Conference on Intelligent Systems and Control (ISCO)*, Jan. 2015, pp. 1–5. doi: 10.1109/ISCO.2015.7282275.
- [42] L. I. Aftanas and S. A. Golocheikine, “Human anterior and frontal midline theta and lower alpha reflect emotionally positive state and internalized attention: high-resolution EEG investigation of meditation,” *Neurosci. Lett.*, vol. 310, no. 1, pp. 57–60, Sep. 2001, doi: 10.1016/S0304-3940(01)02094-8.
- [43] L. I. Aftanas, A. A. Varlamov, S. V. Pavlov, V. P. Makhnev, and N. V. Reva, “Time-dependent cortical asymmetries induced by emotional arousal: EEG analysis of event-related synchronization and desynchronization in individually defined frequency bands,” *Int. J. Psychophysiol.*, vol. 44, no. 1, pp. 67–82, Apr. 2002, doi: 10.1016/S0167-8760(01)00194-5.

- [44] C. S. Nayak and A. C. Anilkumar, "EEG Normal Waveforms," in *StatPearls*, Treasure Island (FL): StatPearls Publishing, 2022. Accessed: Aug. 02, 2022. [Online]. Available: <http://www.ncbi.nlm.nih.gov/books/NBK539805/>
- [45] P. A. Abhang, B. W. Gawali, and S. C. Mehrotra, *Introduction to EEG- and speech-based emotion recognition*. London, UK ; San Diego, CA, USA: Elsevier/AP, Academic Press is an imprint of Elsevier, 2016.
- [46] P. J. Fitzgerald and B. O. Watson, "Gamma oscillations as a biomarker for major depression: an emerging topic," *Transl. Psychiatry*, vol. 8, no. 1, Art. no. 1, Sep. 2018, doi: 10.1038/s41398-018-0239-y.
- [47] R. Vallat, "Compute the average bandpower of an EEG signal." <https://raphaelvallat.com/bandpower.html>
- [48] G. Garcia-Molina, "Direct brain-computer communication through scalp recorded EEG signals," Jan. 2004, doi: 10.5075/epfl-thesis-3019.
- [49] D. F. Hermens *et al.*, "Anorexia nervosa, zinc deficiency and the glutamate system: The ketamine option," *Prog. Neuropsychopharmacol. Biol. Psychiatry*, vol. 101, p. 109921, Jul. 2020, doi: 10.1016/j.pnpbp.2020.109921.
- [50] C. Phillips, "Brain-Derived Neurotrophic Factor, Depression, and Physical Activity: Making the Neuroplastic Connection," *Neural Plast.*, vol. 2017, p. e7260130, Aug. 2017, doi: 10.1155/2017/7260130.
- [51] V. Krishnan and E. J. Nestler, "The molecular neurobiology of depression," *Nature*, vol. 455, no. 7215, Art. no. 7215, Oct. 2008, doi: 10.1038/nature07455.
- [52] A. L. Teixeira, I. G. Barbosa, B. S. Diniz, and A. Kummer, "Circulating levels of brain-derived neurotrophic factor: correlation with mood, cognition and motor function," *Biomark. Med.*, vol. 4, no. 6, pp. 871–887, Dec. 2010, doi: 10.2217/bmm.10.111.
- [53] B.-H. Lee, H. Kim, S.-H. Park, and Y.-K. Kim, "Decreased plasma BDNF level in depressive patients," *J. Affect. Disord.*, vol. 101, no. 1, pp. 239–244, Aug. 2007, doi: 10.1016/j.jad.2006.11.005.
- [54] T. Yoshida *et al.*, "Decreased Serum Levels of Mature Brain-Derived Neurotrophic Factor (BDNF), but Not Its Precursor proBDNF, in Patients with Major Depressive Disorder," *PLOS ONE*, vol. 7, no. 8, p. e42676, Aug. 2012, doi: 10.1371/journal.pone.0042676.
- [55] Y.-K. Kim *et al.*, "Low plasma BDNF is associated with suicidal behavior in major depression," *Prog. Neuropsychopharmacol. Biol. Psychiatry*, vol. 31, no. 1, pp. 78–85, Jan. 2007, doi: 10.1016/j.pnpbp.2006.06.024.
- [56] T. K. Birkenhäger, S. Geldermans, W. W. Van den Broek, N. van Beveren, and D. Fekkes, "Serum brain-derived neurotrophic factor level in relation to illness severity and episode duration in patients with major depression," *J. Psychiatr. Res.*, vol. 46, no. 3, pp. 285–289, Mar. 2012, doi: 10.1016/j.jpsychires.2011.12.006.
- [57] M. L. Molendijk, P. Spinhoven, M. Polak, B. a. A. Bus, B. W. J. H. Penninx, and B. M. Elzinga, "Serum BDNF concentrations as peripheral manifestations of depression: evidence from a systematic review and meta-analyses on 179 associations (N=9484)," *Mol. Psychiatry*, vol. 19, no. 7, Art. no. 7, Jul. 2014, doi: 10.1038/mp.2013.105.
- [58] F. Matrisciano *et al.*, "Changes in BDNF serum levels in patients with major depression disorder (MDD) after 6 months treatment with sertraline, escitalopram, or venlafaxine," *J. Psychiatr. Res.*, vol. 43, no. 3, pp. 247–254, Jan. 2009, doi: 10.1016/j.jpsychires.2008.03.014.

- [59] E. Y.-C. Ting, A. C. Yang, and S.-J. Tsai, "Role of Interleukin-6 in Depressive Disorder," *Int. J. Mol. Sci.*, vol. 21, no. 6, p. 2194, Mar. 2020, doi: 10.3390/ijms21062194.
- [60] N. Rohleder, "Stimulation of Systemic Low-Grade Inflammation by Psychosocial Stress," *Psychosom. Med.*, vol. 76, no. 3, pp. 181–189, Apr. 2014, doi: 10.1097/PSY.0000000000000049.
- [61] Y. Dowlati *et al.*, "A Meta-Analysis of Cytokines in Major Depression," *Biol. Psychiatry*, vol. 67, no. 5, pp. 446–457, Mar. 2010, doi: 10.1016/j.biopsych.2009.09.033.
- [62] M. B. Howren, D. M. Lamkin, and J. Suls, "Associations of Depression With C-Reactive Protein, IL-1, and IL-6: A Meta-Analysis," *Psychosom. Med.*, vol. 71, no. 2, pp. 171–186, Mar. 2009, doi: 10.1097/PSY.0b013e3181907c1b.
- [63] Y. Liu, R. C.-M. Ho, and A. Mak, "Interleukin (IL)-6, tumour necrosis factor alpha (TNF- α) and soluble interleukin-2 receptors (sIL-2R) are elevated in patients with major depressive disorder: A meta-analysis and meta-regression," *J. Affect. Disord.*, vol. 139, no. 3, pp. 230–239, Aug. 2012, doi: 10.1016/j.jad.2011.08.003.
- [64] D. D. Kiraly *et al.*, "Altered peripheral immune profiles in treatment-resistant depression: response to ketamine and prediction of treatment outcome," *Transl. Psychiatry*, vol. 7, no. 3, Art. no. 3, Mar. 2017, doi: 10.1038/tp.2017.31.
- [65] F. Lederbogen, B. Weber, M. Colla, I. Heuser, and M. Deuschle, "Endothelin-1 Plasma Concentrations in Depressed Patients and Healthy Controls," *Neuropsychobiology*, vol. 40, no. 3, pp. 121–123, 1999, doi: 10.1159/000026607.
- [66] M. M. Burg, E. J. Martens, D. Collins, and R. Soufer, "Depression Predicts Elevated Endothelin-1 in Patients with Coronary Artery Disease," *Psychosom. Med.*, vol. 73, no. 1, pp. 2–6, Jan. 2011, doi: 10.1097/PSY.0b013e3181fdfb25.
- [67] M. Jobert *et al.*, "Guidelines for the Recording and Evaluation of PharmacoeEG Data in Man: The International PharmacoeEG Society (IPEG)," *Neuropsychobiology*, vol. 66, no. 4, pp. 201–220, 2012, doi: 10.1159/000343478.
- [68] E. C. Ifeachor and B. W. Jervis, *Digital Signal Processing: A Practical Approach*, 2nd ed. Pearson Education, 2002.
- [69] A. Widmann, E. Schröger, and B. Maess, "Digital filter design for electrophysiological data – a practical approach," *J. Neurosci. Methods*, vol. 250, pp. 34–46, Jul. 2015, doi: 10.1016/j.jneumeth.2014.08.002.
- [70] M. A. Uusitalo and R. J. Ilmoniemi, "Signal-space projection method for separating MEG or EEG into components," *Med. Biol. Eng. Comput.*, vol. 35, no. 2, pp. 135–140, Mar. 1997, doi: 10.1007/BF02534144.
- [71] A. Gramfort *et al.*, "MEG and EEG data analysis with MNE-Python," *Front. Neurosci.*, vol. 7, 2013, Accessed: Aug. 04, 2022. [Online]. Available: <https://www.frontiersin.org/articles/10.3389/fnins.2013.00267>
- [72] M. Jas, D. Engemann, F. Raimondo, Y. Bekhti, and A. Gramfort, "Automated rejection and repair of bad trials in MEG/EEG," in *6th International Workshop on Pattern Recognition in Neuroimaging (PRNI)*, Trento, Italy, Jun. 2016. Accessed: Aug. 04, 2022. [Online]. Available: <https://hal.archives-ouvertes.fr/hal-01313458>
- [73] M. Jas, D. A. Engemann, Y. Bekhti, F. Raimondo, and A. Gramfort, "Autoreject: Automated artifact rejection for MEG and EEG data," *NeuroImage*, vol. 159, pp. 417–429, Oct. 2017, doi: 10.1016/j.neuroimage.2017.06.030.
- [74] P. Welch, "The use of fast Fourier transform for the estimation of power spectra: A method based on time averaging over short, modified periodograms," *IEEE Trans. Audio Electroacoustics*, vol. 15, no. 2, pp. 70–73, Jun. 1967, doi: 10.1109/TAU.1967.1161901.

- [75] C. Leys, C. Ley, O. Klein, P. Bernard, and L. Licata, “Detecting outliers: Do not use standard deviation around the mean, use absolute deviation around the median,” *J. Exp. Soc. Psychol.*, vol. 49, no. 4, pp. 764–766, Jul. 2013, doi: 10.1016/j.jesp.2013.03.013.
- [76] M. Mukaka, “A guide to appropriate use of Correlation coefficient in medical research,” *Malawi Med. J. J. Med. Assoc. Malawi*, vol. 24, no. 3, pp. 69–71, Sep. 2012.
- [77] W. McKinney, “Data Structures for Statistical Computing in Python,” presented at the Python in Science Conference, Austin, Texas, 2010, pp. 56–61. doi: 10.25080/Majora-92bf1922-00a.
- [78] J. Reback *et al.*, “pandas-dev/pandas: Pandas 1.4.3.” Zenodo, Jun. 23, 2022. doi: 10.5281/ZENODO.3509134.
- [79] C. R. Harris *et al.*, “Array programming with NumPy,” *Nature*, vol. 585, no. 7825, Art. no. 7825, Sep. 2020, doi: 10.1038/s41586-020-2649-2.
- [80] P. Virtanen *et al.*, “SciPy 1.0: fundamental algorithms for scientific computing in Python,” *Nat. Methods*, vol. 17, no. 3, pp. 261–272, Mar. 2020, doi: 10.1038/s41592-019-0686-2.
- [81] J. D. Hunter, “Matplotlib: A 2D Graphics Environment,” *Comput. Sci. Eng.*, vol. 9, no. 3, pp. 90–95, May 2007, doi: 10.1109/MCSE.2007.55.
- [82] T. A. Caswell *et al.*, “matplotlib/matplotlib: REL: v3.5.2.” Zenodo, May 03, 2022. doi: 10.5281/ZENODO.592536.
- [83] M. Waskom, “seaborn: statistical data visualization,” *J. Open Source Softw.*, vol. 6, no. 60, p. 3021, Apr. 2021, doi: 10.21105/joss.03021.
- [84] V. Pupovac and M. Petrovečki, “Summarizing and presenting numerical data,” *Biochem. Medica*, vol. 21, no. 2, pp. 106–110, Jun. 2011, doi: 10.11613/BM.2011.018.
- [85] H. M. Bu-Omer, A. Gofuku, K. Sato, and M. Miyakoshi, “Parieto-Occipital Alpha and Low-Beta EEG Power Reflect Sense of Agency,” *Brain Sci.*, vol. 11, no. 6, Art. no. 6, Jun. 2021, doi: 10.3390/brainsci11060743.
- [86] P. Haggard, “Sense of agency in the human brain,” *Nat. Rev. Neurosci.*, vol. 18, no. 4, Art. no. 4, Apr. 2017, doi: 10.1038/nrn.2017.14.
- [87] K. H. Bentley, J. C. Franklin, J. D. Ribeiro, E. M. Kleiman, K. R. Fox, and M. K. Nock, “Anxiety and its disorders as risk factors for suicidal thoughts and behaviors: A meta-analytic review,” *Clin. Psychol. Rev.*, vol. 43, pp. 30–46, Feb. 2016, doi: 10.1016/j.cpr.2015.11.008.

Appendix 1 – Non-exclusive licence for reproduction and publication of a thesis¹

I, Toomas Erik Anijärv

1. Grant Tallinn University of Technology free licence (non-exclusive licence) for my thesis “Long-term electrophysiological changes and relationship with clinical and biochemical measures following a 6-week low-dose oral ketamine treatment in adults with major depressive disorder and chronic suicidality”, supervised by Prof. Jim Lagopoulos and Prof. Maie Bachmann.
 - 1.1. to be reproduced for the purposes of preservation and electronic publication of the graduation thesis, incl. to be entered in the digital collection of the library of Tallinn University of Technology until expiry of the term of copyright;
 - 1.2. to be published via the web of Tallinn University of Technology, incl. to be entered in the digital collection of the library of Tallinn University of Technology until expiry of the term of copyright.
2. I am aware that the author also retains the rights specified in clause 1 of the non-exclusive licence.
3. I confirm that granting the non-exclusive licence does not infringe other persons' intellectual property rights, the rights arising from the Personal Data Protection Act or rights arising from other legislation.

03.01.2023

¹ The non-exclusive licence is not valid during the validity of access restriction indicated in the student's application for restriction on access to the graduation thesis that has been signed by the school's dean, except in case of the university's right to reproduce the thesis for preservation purposes only. If a graduation thesis is based on the joint creative activity of two or more persons and the co-author(s) has/have not granted, by the set deadline, the student defending his/her graduation thesis consent to reproduce and publish the graduation thesis in compliance with clauses 1.1 and 1.2 of the non-exclusive licence, the non-exclusive license shall not be valid for the period.

Appendix 2 – Demographics table of the participants

Table 2. Demographics, diagnosis, concurrent medications, and gathered data of the subjects (* ‘in addition to Chronic Suicidality’)

Subject	Data acquisition	Gender	Age, years	DSM-5 diagnosis*	Psychotropic medication(s)
01	EEG + blood test	Male	63.16	MDD, GAD	Quetiapine, Tranylcypromine, Chlorpromazine
02	EEG + blood test	Male	32.35	MDD, GAD	Escitalopram
03	EEG + blood test	Female	45.62	MDD	Sertraline
06	EEG + blood test	Female	58.63	MDD, GAD	Quetiapine, Lithium, Imipramine, Chlorpromazine
07	EEG + blood test	Male	42.34	MDD, GAD	Escitalopram, Propranolol
08	EEG + blood test	Male	63.71	MDD, GAD	Sertraline
10	EEG + blood test	Female	22.19	MDD, GAD	Fluoxetine
11	EEG + blood test	Male	47.30	MDD	Duloxetine, Mirtazapine, Pregabalin
12	EEG + blood test	Female	27.17	MDD, GAD, BPD	Vortioxetine, Valium, Fluoxetine
15	EEG	Female	50.23	MDD	Asenapine, Lithium, Sertraline, Bupropion
16	EEG	Male	58.33	MDD	Amitriptyline
18	EEG + blood test	Male	30.21	OCD, MDD	-
20	EEG + blood test	Male	48.34	MDD, PTSD	Olanzapine, Mirtazapine, Duloxetine
22	EEG + blood test	Male	45.62	MDD, PTSD	Desvenlafaxine, Mirtazapine, Lithium
23	EEG	Female	30.51	MDD, BPD	Paroxetine
25	EEG + blood test	Female	36.04	MDD, GAD, BPD	Duloxetine, Lithium, Lorazepam
26	EEG + blood test	Female	55.70	OCD, PTSD, MDD	-
27	EEG + blood test	Male	64.06	GAD, MDD	Lithium, Clomipramine, Olanzapine, Zolpidem, Asenapine
28	EEG + blood test	Female	57.65	MDD, GAD	Duloxetine, Amitriptyline
29	EEG + blood test	Male	71.80	MDD	-
31	EEG	Female	38.71	MDD, GAD	Sertraline, Quetiapine
33	EEG	Female	33.33	MDD, GAD, BPD, SUD	Fluoxetine, Asenapine
35	EEG + blood test	Female	55.86	MDD	Fluoxetine
38	EEG + blood test	Female	24.11	MDD, GAD	Duloxetine, Amitriptyline, Pregabalin
40	EEG + blood test	Female	57.19	MDD, PTSD	Oxazepam

Appendix 3 – Tables for band powers and comparisons across timepoints

Table 3. Theta band power descriptive values for different timepoints and brain regions with statistical significance levels for comparisons (* $p < .05$; ** $p < .01$).

	Baseline		6 weeks		10 weeks		Comparison		
	Mean (SD)	Median (IQR)	Mean (SD)	Median (IQR)	Mean (SD)	Median (IQR)	p ₀₋₆	p ₆₋₁₀	p ₀₋₁₀
Frontal	2.227 (3.251)	1.375 (0.743-2.677)	1.680 (1.590)	1.111 (0.638-1.769)	1.814 (1.782)	1.218 (0.699-2.397)	0.220	0.287	0.396
Temporal	3.453 (3.698)	2.252 (1.387-3.762)	3.018 (2.173)	2.641 (1.194-4.694)	3.763 (2.939)	2.784 (1.334-5.932)	0.634	0.006**	0.090
Centro-parietal	1.286 (1.353)	0.853 (0.559-1.449)	1.145 (0.939)	0.857 (0.399-1.492)	1.268 (1.006)	1.025 (0.437-1.698)	0.751	0.019*	0.508
Occipital	3.899 (3.986)	2.630 (1.612-4.236)	3.410 (2.525)	3.670 (1.189-5.140)	3.986 (3.136)	2.854 (1.375-5.874)	0.525	0.012*	0.312

Table 4. Alpha band power descriptive values for different timepoints and brain regions with statistical significance levels for comparisons (* $p < .05$; ** $p < .01$).

	Baseline		6 weeks		10 weeks		Comparison		
	Mean (SD)	Median (IQR)	Mean (SD)	Median (IQR)	Mean (SD)	Median (IQR)	p ₀₋₆	p ₆₋₁₀	p ₀₋₁₀
Frontal	2.556 (2.193)	1.328 (0.867-3.755)	2.107 (1.964)	1.343 (0.820-2.613)	2.543 (2.343)	1.738 (0.759-3.439)	0.381	0.200	0.596
Temporal	5.513 (4.505)	4.302 (1.999-8.163)	4.408 (2.952)	3.989 (2.263-5.742)	6.288 (5.264)	4.130 (3.321-8.034)	0.173	0.003**	0.113
Centro-parietal	2.509 (2.017)	2.248 (0.758-3.605)	1.937 (1.361)	1.635 (0.871-3.077)	2.522 (2.068)	2.004 (1.109-3.574)	0.048*	0.007**	0.634
Occipital	11.417 (15.845)	5.802 (3.177-13.386)	9.316 (11.217)	6.499 (3.066-9.136)	12.914 (16.872)	8.094 (4.424-12.789)	0.411	0.113	0.287

Table 5. Low-Beta band power descriptive values for different timepoints and brain regions with statistical significance levels for comparisons (* $p < .05$).

	Baseline		6 weeks		10 weeks		Comparison		
	Mean (SD)	Median (IQR)	Mean (SD)	Median (IQR)	Mean (SD)	Median (IQR)	p ₀₋₆	p ₆₋₁₀	p ₀₋₁₀

Frontal	0.713 (0.525)	0.544 (0.305- 0.938)	0.559 (0.342)	0.403 (0.300- 0.749)	0.593 (0.428)	0.435 (0.301- 0.833)	0.113	0.634	0.141
Temporal	1.367 (1.009)	1.043 (0.731- 1.508)	1.202 (0.673)	1.042 (0.701- 1.388)	1.449 (1.114)	0.953 (0.781- 1.665)	0.751	0.042*	0.396
Centro- parietal	0.602 (0.544)	0.510 (0.257- 0.704)	0.492 (0.393)	0.390 (0.284- 0.550)	0.572 (0.540)	0.414 (0.218- 0.701)	0.134	0.252	0.895
Occipital	1.712 (1.297)	1.167 (0.865- 2.135)	1.517 (1.231)	0.987 (0.708- 2.297)	1.885 (1.743)	1.170 (0.767- 2.224)	0.353	0.027*	0.312

Table 6. High-Beta band power descriptive values for different timepoints and brain regions with statistical significance levels for comparisons.

	Baseline		6 weeks		10 weeks		Comparison		
	Mean (SD)	Median (IQR)	Mean (SD)	Median (IQR)	Mean (SD)	Median (IQR)	P0-6	P6-10	P0-10
Frontal	0.490 (0.441)	0.353 (0.213- 0.534)	0.390 (0.270)	0.335 (0.151- 0.513)	0.373 (0.258)	0.294 (0.228- 0.489)	0.312	1.000	0.426
Temporal	0.679 (0.537)	0.473 (0.389- 0.789)	0.628 (0.427)	0.468 (0.345- 0.771)	0.695 (0.494)	0.545 (0.430- 0.758)	0.958	0.263	0.474
Centro- parietal	0.285 (0.247)	0.221 (0.150- 0.288)	0.241 (0.171)	0.176 (0.152- 0.281)	0.279 (0.275)	0.188 (0.138- 0.317)	0.275	0.300	0.937
Occipital	0.710 (0.636)	0.469 (0.384- 0.889)	0.604 (0.443)	0.415 (0.310- 0.831)	0.835 (0.939)	0.537 (0.345- 1.133)	0.230	0.156	0.325

Appendix 4 – Correlation tables between band powers and clinical outcomes

Table 7. Theta band power correlation coefficients with clinical outcomes for different timepoints and brain regions (* p<.05; ** p<.01, *** p<.001).

	Baseline - 6 weeks				6 weeks - 10 weeks				Baseline - 10 weeks			
	BSS	DASS (D)	DASS (A)	DASS (S)	BSS	DASS (D)	DASS (A)	DASS (S)	BSS	DASS (D)	DASS (A)	DASS (S)
Frontal	-0.027	-0.177	-0.076	-0.205	-0.056	-0.313	-0.055	-0.132	0.033	-0.046	0.024	-0.113
Temporal	-0.305	-0.289	-0.377	-0.585 **	-0.044	0.143	-0.055	0.099	0.102	-0.064	-0.283	-0.062
Centro-parietal	-0.088	-0.313	-0.221	-0.299	0.128	-0.072	-0.198	0.039	0.058	-0.150	-0.404 *	-0.139
Occipital	-0.309	-0.358	-0.522 **	-0.659 ***	0.162	0.431 *	0.235	0.526 **	0.084	-0.111	-0.235	0.014

Table 8. Alpha band power correlation coefficients with clinical outcomes for different timepoints and brain regions (* p<.05).

	Baseline - 6 weeks				6 weeks - 10 weeks				Baseline - 10 weeks			
	BSS	DASS (D)	DASS (A)	DASS (S)	BSS	DASS (D)	DASS (A)	DASS (S)	BSS	DASS (D)	DASS (A)	DASS (S)
Frontal	0.005	-0.056	0.029	-0.150	0.011	-0.376	-0.241	-0.372	-0.088	-0.130	0.057	-0.189
Temporal	-0.143	-0.159	-0.231	-0.358	0.100	0.213	0.278	0.110	-0.109	-0.196	-0.455 *	-0.402 *
Centro-parietal	0.089	-0.115	-0.053	-0.120	0.312	0.055	0.150	0.083	0.008	-0.092	-0.349	-0.248
Occipital	-0.058	-0.108	-0.152	-0.222	0.015	0.286	0.310	0.229	-0.156	-0.305	-0.284	-0.335

Table 9. Low-beta band power correlation coefficients with clinical outcomes f for different timepoints and brain regions (* p<.05; ** p<.01).

	Baseline - 6 weeks				6 weeks - 10 weeks				Baseline - 10 weeks			
	BSS	DASS (D)	DASS (A)	DASS (S)	BSS	DASS (D)	DASS (A)	DASS (S)	BSS	DASS (D)	DASS (A)	DASS (S)
Frontal	0.012	-0.190	0.067	-0.176	-0.151	-0.464 *	-0.224	-0.375	-0.057	-0.203	0.032	-0.288
Temporal	-0.394	-0.356	-0.251	-0.528 **	-0.151	-0.024	0.006	-0.078	-0.256	-0.384	-0.375	-0.331
Centro-parietal	-0.106	-0.276	-0.152	-0.312	0.009	-0.032	0.044	0.053	-0.044	-0.284	-0.336	-0.171
Occipital	-0.248	-0.249	-0.234	-0.506 **	0.044	0.379	0.169	0.318	-0.149	-0.421 *	-0.282	-0.216

Table 10. High-beta band power correlation coefficients with clinical outcomes for different timepoints and brain regions (* p<.05; ** p<.01).

	Baseline - 6 weeks				6 weeks - 10 weeks				Baseline - 10 weeks			
	BSS	DASS (D)	DASS (A)	DASS (S)	BSS	DASS (D)	DASS (A)	DASS (S)	BSS	DASS (D)	DASS (A)	DASS (S)
Frontal	0.097	0.030	0.315	0.055	-0.388	-0.571 **	-0.211	-0.365	0.075	-0.070	0.215	-0.181
Temporal	-0.324	-0.227	-0.033	-0.334	-0.215	-0.120	0.176	-0.073	-0.365	-0.504 *	-0.443 *	-0.595 **
Centro-parietal	-0.093	-0.092	0.181	-0.165	-0.008	-0.101	0.114	-0.029	-0.186	-0.420 *	-0.181	-0.204
Occipital	-0.228	-0.167	-0.159	-0.391	-0.130	0.135	-0.006	0.051	-0.236	-0.396	-0.364	-0.399 *

Appendix 5 – Correlation tables between band powers and biochemical measures

Table 11. Theta band power correlation coefficients with biochemical measures for different timepoints and brain regions (* p<.05; ** p<.01).

	Baseline - 6 weeks			6 weeks - 10 weeks			Baseline - 10 weeks		
	BDNF	IL-6	ET-1	BDNF	IL-6	ET-1	BDNF	IL-6	ET-1
Frontal	0.265	0.519 *	0.307	-0.024	0.238	0.347	0.086	-0.030	0.038
Temporal	0.235	0.496 *	0.565 **	-0.026	0.053	0.149	-0.057	0.152	0.147
Centro- parietal	0.096	0.651 **	0.355	-0.478 *	0.141	0.170	-0.146	-0.036	0.153
Occipital	0.170	0.182	0.477 *	-0.203	0.117	0.092	0.081	0.202	0.035

Table 12. Alpha band power correlation coefficients with biochemical measures for different timepoints and brain regions (* p<.05; ** p<.01).

	Baseline - 6 weeks			6 weeks - 10 weeks			Baseline - 10 weeks		
	BDNF	IL-6	ET-1	BDNF	IL-6	ET-1	BDNF	IL-6	ET-1
Frontal	0.338	0.568 **	0.289	-0.144	-0.119	0.168	0.211	-0.131	-0.156
Temporal	-0.012	0.191	0.194	-0.078	0.173	-0.120	0.054	0.003	0.092
Centro- parietal	0.026	0.534 *	-0.033	-0.223	-0.006	0.186	-0.177	-0.077	0.027
Occipital	-0.093	0.182	0.135	-0.014	0.138	-0.314	0.296	0.198	0.009

Table 13. Low-beta band power correlation coefficients with biochemical measures for different timepoints and brain regions (* p<.05; ** p<.01).

	Baseline - 6 weeks			6 weeks - 10 weeks			Baseline - 10 weeks		
	BDNF	IL-6	ET-1	BDNF	IL-6	ET-1	BDNF	IL-6	ET-1
Frontal	0.095	0.677 **	0.295	-0.149	-0.107	0.194	0.080	-0.194	-0.123
Temporal	0.099	0.481 *	0.353	-0.008	-0.113	-0.011	0.092	-0.063	-0.128
Centro- parietal	0.117	0.549 *	0.104	-0.426	-0.218	0.060	-0.135	-0.102	-0.176
Occipital	0.176	0.241	0.296	-0.298	-0.128	-0.183	-0.075	0.062	-0.164

Table 14. High-beta band power correlation coefficients with biochemical measures for different timepoints and brain regions (* p<.05).

	Baseline - 6 weeks			6 weeks - 10 weeks			Baseline - 10 weeks		
	BDNF	IL-6	ET-1	BDNF	IL-6	ET-1	BDNF	IL-6	ET-1
Frontal	-0.200	0.552 *	0.107	-0.174	-0.141	-0.053	0.002	-0.150	-0.140
Temporal	-0.250	0.389	0.223	0.134	-0.205	-0.171	0.117	0.048	0.224
Centro- parietal	-0.158	0.537 *	0.164	-0.250	-0.205	0.029	-0.141	-0.131	-0.048
Occipital	-0.191	0.165	0.065	-0.248	-0.111	-0.418	-0.005	0.205	0.165